Cell-Deposited Matrix Improves Retinal Pigment Epithelium Survival on Aged Submacular Human Bruch's Membrane

Ilene K. Sugino,[1] Vamsi K. Gullapalli,[1] Qian Sun,[1] Jianqiu Wang,[1] Celia F. Nunes,[1] Nooounanong Cheewatrakoolpong,[1] Adam C. Johnson,[1] Benjamin C. Degner,[1] Jianyuan Hua,[1] Tong Liu,[2] Wei Chen,[2] Hong Li,[2] and Marco A. Zarbin[1]

Purpose. To determine whether resurfacing submacular human Bruch's membrane with a cell-deposited extracellular matrix (ECM) improves retinal pigment epithelial (RPE) survival.

Methods. Bovine corneal endothelial (BCE) cells were seeded onto the inner collagenous layer of submacular Bruch's membrane explants of human donor eyes to allow ECM deposition. Control explants from fellow eyes were cultured in medium only. The deposited ECM was exposed by removing BCE. Fetal RPE cells were then cultured on these explants for 1, 14, or 21 days. The explants were analyzed quantitatively by light microscopy and scanning electron microscopy. Surviving RPE cells from explants cultured for 21 days were harvested to compare bestrophin and RPE65 mRNA expression. Mass spectroscopy was performed on BCE-ECM to examine the protein composition.

Results. The BCE-treated explants showed significantly higher RPE nuclear density than did the control explants at all time points. RPE expressed more differentiated features on BCE-treated explants than on untreated explants, but expressed very little mRNA for bestrophin or RPE65. The untreated young (<50 years) and African American submacular Bruch's membrane explants supported significantly higher RPE nuclear densities (NDs) than did the Caucasian explants. These differences were reduced or nonexistent in the BCE-ECM-treated explants. Proteins identified in the BCE-ECM included ECM proteins, ECM-associated proteins, cell membrane proteins, and intracellular proteins.

Conclusions. Increased RPE survival can be achieved on aged submacular human Bruch's membrane by resurfacing the latter with a cell-deposited ECM. Caucasian eyes seem to benefit the most, as cell survival is the worst on submacular Bruch's membrane in these eyes. (*Invest Ophthalmol Vis Sci.* 2011;52:1345–1358) DOI:10.1167/iovs.10-6112

There is no fully effective therapy for the late complications of age-related macular degeneration (AMD), the leading cause of blindness in the United States. The prevalence of AMD-associated choroidal new vessels (CNVs) and/or geographic atrophy (GA) in the U.S. population 40 years and older is estimated to be 1.47%, with 1.75 million citizens having advanced AMD, approximately 100,000 of whom are African American.[1] The prevalence of AMD increases dramatically with age, with more than 10% of persons older than 80 years having CNVs and/or GA.[1] More than 7 million individuals have drusen measuring 125 μm or larger and are therefore at substantial risk of developing AMD.[1] Due to the rapidly aging population, the number of persons having AMD will increase to 2.95 million in 2020.[1] Therapy that blocks the effects of vascular endothelial growth factor is the best treatment available for CNVs currently, but randomized studies indicate that only 30% and 40% of treated patients experience at least moderate visual improvement.[2,3] There is no proven therapy for GA.[4] Compared to pharmacologic monotherapy, cell-based therapy has the potential advantage of providing long-term clinical benefit without the need for frequently repeated minor surgical treatments or long-term administration of medications. Furthermore, cells such as RPE cells can produce many factors[5–11] (e.g., PEDF, bFGF, VEGF, angiopoietin, and HIF-1) that help preserve normal retinal and choroidal anatomy and physiology. Thus, in principle, cell-based therapy may offer a richer, more effective therapy to AMD patients than current pharmacologic therapy. Potential benefits of the pharmacologic complexity of cell-based therapy include less chance for emergence of resistance to treatment or failure to respond to treatment, and greater chance for visual recovery (e.g., due to production of neurotrophic factors by RPE cells). Although it is not proved, we hope that cell-based therapy for AMD will offer the same relative benefit to patients as pancreatic islet cell transplants offer to patients with diabetes (compared with therapy using insulin pumps).

There is abundant preclinical evidence that cell-based therapy can prevent photoreceptor degeneration in conditions associated with RPE dysfunction—for example, the Royal College of Surgeons rat (please see Gullapalli et al.[12] for a review),[13,14] whose RPE has a mutation in *mertk*, and RPE-65 mutant mice,[15,16] as well as in a mouse model of Stargardt disease,[17] in which the primary defect is in a photoreceptor protein but in which the RPE are secondarily affected and degenerate. Although the inciting events in AMD may or may not involve the RPE directly,[18–34] ultimately these cells are

From the [1]The Institute of Ophthalmology and Visual Science and the [2]Center for Advanced Proteomics Research, New Jersey Medical School, University of Medicine and Dentistry of New Jersey (UMDNJ), Newark, New Jersey.

Supported in part by National Institutes of Health Grant R03 EY013690, P30NS046593 (HL); the Foundation Fighting Blindness; the Lincy Foundation; an unrestricted grant from Research to Prevent Blindness; The Eye Institute of New Jersey; the Janice Mitchell Vassar and Ashby John Mitchell Fellowship; the Joseph J. and Marguerite DiSepio Retina Research Fund; the Foundation of UMDNJ; and the New Jersey Lions Eye Research Foundation.

Submitted for publication June 23, 2010; revised August 29, 2010; accepted October 14, 2010.

Disclosure: **I.K. Sugino**, P; **V.K. Gullapalli**, P; **Q. Sun**, None; **J. Wang**, None; **C.F. Nunes**, None; **B. Degner**, None; **N. Cheewatrakoolpong**, None; **A.C. Johnson**, None; **J. Hua**, None; **T. Liu**, None; **W. Chen**, None; **H. Li**, None; **M.A. Zarbin**, P

Corresponding author: Marco A. Zarbin, UMDNJ-New Jersey Medical School, Institute of Ophthalmology and Visual Science, DOC 6th Floor, 90 Bergen Street, Newark, NJ 07101-1709; zarbin@umdnj.edu.

damaged with associated formation of drusen, GA, and CNVs. Laboratory experiments link RPE lipofuscin, oxidative damage, drusen, and inflammation, all of which have been implicated in AMD pathogenesis.[35–38] Although cell-based therapy has been effective in animal models of retinal degeneration, including models that mimic aspects of AMD,[15,17,39,40] trials of RPE transplants in AMD patients have been largely unsuccessful.[41–46] Studies of RPE attachment and survival on human aged submacular Bruch's membrane indicate that transplanted RPE cells do not survive in the long-term on this substrate.[47,48]

The age- and AMD-induced modification of Bruch's membrane may explain the discrepancy in the outcomes of human versus animal RPE transplantation.[48] With normal aging, human Bruch's membrane, especially in the submacular region, undergoes numerous changes (e.g., increased thickness, deposition of lipids, cross-linking of proteins, and nonenzymatic formation of advanced glycation end products).[35,49] These changes and additional changes due to AMD could decrease the bioavailability of extracellular matrix (ECM) proteins (e.g., laminin, fibronectin, collagen IV, proteoglycans, and growth factors),[50] resulting in limited cell–matrix interactions and poor survival and differentiation of transplanted RPE cells in AMD eyes. Because the changes in Bruch's membrane from aging and AMD are complex and may not be fully reversible, one approach is to establish a new ECM over Bruch's membrane. In one study, the addition of ECM ligands, singly or in combination (e.g., combinations of laminin, fibronectin, vitronectin, and collagen IV), to aged human Bruch's membrane improved initial RPE attachment to a limited degree.[51] Detergent treatment of Bruch's membrane followed by soluble ECM protein application improved long-term cell survival to a limited degree, but cell morphology was abnormal.[52] The modest RPE survival in these studies was observed on peripheral Bruch's membrane where there is a lesser degree of age- and AMD-related change.[35] Similarly, RPE resurfacing on culture plates coated with single ligands is poor compared with that on a cell-secreted matrix.[53] Single soluble ECM ligands or a combination of soluble ECM molecules do not necessarily replicate the complexity of a cell-deposited ECM.

The goal of the present study was to determine whether coating aged human submacular Bruch's membrane with a cell-secreted ECM improves transplanted RPE survival over a relatively long period (i.e., 3 weeks, versus attachment and survival for 24 hours after seeding, which has been assessed by previous investigators). RPE behavior was studied on aged submacular Bruch's membrane resurfaced by an ECM deposited by bovine corneal endothelial cells (BCE-ECM). This matrix was chosen because BCE-ECM-coated tissue culture dishes support rapid attachment, growth, and differentiation of RPE cells in culture.[54] We hypothesized that the complex three-dimensional BCE-ECM could support cells to a greater degree than was observed with application of soluble ligands. Mass spectroscopy was performed on solubilized BCE-ECM to determine the major protein components. Although the approach to reconstructing a suitable extracellular environment described in this study is not practical for clinical treatment of AMD patients, these studies demonstrate that resurfacing aged submacular human Bruch's membrane with a complex cell-secreted ECM can improve cell survival and differentiation greatly.

Materials and Methods

Studies involving use of human donor tissue adhered to the tenets of the Declaration of Helsinki and were approved by the institutional review board of the University of Medicine and Dentistry of New Jersey.

Bruch's Membrane Preparation

Adult donor eyes (ages, 41–86 years; Table 1) were received from the Lions Eye Institute for Transplant and Research (Tampa, FL) and eyebanks placing donor eyes through their website (Ocular Research Biologics System [ORBS], http://www.orbsproject.org), Midwest Eyebanks (includes eyebanks in Illinois, Michigan, and New Jersey), the San Diego Eyebank (San Diego, CA), and eyebanks placing tissue through the National Disease Research Interchange (NDRI, Philadelphia, PA). Acceptance criteria for donor eyes included: death-to-enucleation time no more than 7 hours, death-to-receipt time no more than 48 hours, no ventilator support before death, no recent chemotherapy (within the past 6 months), no recent radiation to the head, no recent head trauma, and no history of conditions affecting the posterior segment (e.g., AMD [with the exception of two patients, one of whom had pigmentary changes and drusen and one of whom had extensive drusen as detailed in Table 1], glaucoma, laser treatment). The donor eyes were immersed in 10% povidone iodine (Betadine solution; Purdue Frederick Co., Norwalk, CT) after removal of extraocular muscles, remnants of conjunctiva, orbital fat, and Tenon's capsule. They were then rinsed in an excess of Dulbecco's modified Eagle's medium (DMEM; Cellgro-Mediatech Inc., Manassas, VA) supplemented with 2.5 μg/mL amphotericin B (Invitrogen-Gibco, Life Technologies, Carlsbad, CA). After the anterior segment, vitreous, and retina were dissected, the donor eyes were examined carefully for submacular disease. A previously published method was used to expose the RPE basement membrane or inner collagenous layer (ICL) surfaces.[47,48,55,56] (RPE basement membrane surfaces were studied for preliminary studies of BCE-ECM deposition only.) Six-millimeter diameter corneal trephines (Bausch & Lomb, Rochester, NY) were used to create macula-centered, round Bruch's membrane explants. These explants were placed in wells of 96-well plates for organ culture.

BCE Culture

Fresh steer eyes were obtained from local meat processors (Animal Parts, Scotch Plains, NJ) within a few hours after death. Corneas were cut from the eyes after sterilization of the corneal surface and surrounding of the tissue by a brief rinse with 70% ethanol. Corneas were positioned with the epithelial surface down on a sterile support placed on a Petri dish, and the endothelial surface was covered with 0.05%

Table 1. Donor Information and Fetal RPE (fRPE) Seeding Density of Paired Bruch's Membrane Explants for Organ Culture at Days 1, 14, and 21

Time Point	Ethnicity	Donor Pairs (*n*)	Mean Donor Age ± SEM (y)	Disease	fRPE Seeding Density (cells/mm^2)
Day 1	Caucasian	7	72.1 ± 3.1	Normal except for one donor with focal RPE hyperpigmentation with associated drusen	885
Day 14	Caucasian	8	72.4 ± 2.6	Normal	3164
Day 21	Caucasian	11	73.9 ± 2.2	Normal	3164
Day 21	African American	6	64.2 ± 4.9	Normal except 1 donor with extensive drusen	3164
Day 21	Young	5	44.8 ± 1.0	Normal	3164

trypsin-EDTA (Invitrogen-Gibco). The corneas were then incubated for 20 minutes at 37°C. BCE cells were isolated by lightly scraping the interior surface of the cornea with a blunt metal spatula and washing with DMEM. Harvested BCE cells were seeded onto 60-mm tissue culture dishes and cultured at 37°C in 10% CO_2 in DMEM (containing 3.7g/L sodium bicarbonate) supplemented with 2 mM glutamine, 15% fetal bovine serum, 2.5 μg/mL amphotericin B, 50 μg/mL gentamicin, and 1 ng/mL bFGF (all from Invitrogen-Gibco) (hereafter referred to as RPE medium).[54] On confluence, the cells were passaged onto 12-well dishes after removal with 0.25% trypsin-EDTA and maintained in culture until seeding onto Bruch's membrane. The cells were removed from 12-well dishes by trypsin-EDTA and seeded at a density of 3164 cells/mm^2 on Bruch's membrane. Passage 2 cells were used for all BCE cell seeding experiments.

BCE Cell Culture on Bruch's Membrane

BCE cells were seeded onto one Bruch's membrane explant of a donor pair and cultured at 37°C in 10% CO_2 in DMEM supplemented with 10% fetal bovine serum, 5% donor calf serum (Invitrogen-Gibco), 2 mM glutamine, 2.5 μg/mL amphotericin B, 50 μg/mL gentamicin, 1 ng/mL bFGF, and 4% dextran (Sigma-Aldrich, St. Louis, MO) (hereafter referred to as ECM medium); 1 ng/mL bFGF was added every other day during the first week of culture. Non-BCE cell-treated controls (i.e., the explant derived from the fellow eye of a donor pair) were maintained in DMEM supplemented with gentamicin and amphotericin only (control medium). BCE cells were removed by soaking the explants in 0.02 M NH_4OH for 5 minutes at room temperature. Cell debris was removed by rinsing for 10 minutes in phosphate buffered saline (PBS) three times. Control explants were treated similarly. Preliminary studies evaluated ECM deposition on submacular RPE basement membrane as well as the surface of the ICL after 7 or 14 days in culture. Of the two surfaces studied and at the two incubation periods, ECM deposition appeared to be the least variable and most tightly adherent to the surface of the ICL (data not shown) after 14-day BCE culture. Therefore, for this study, Bruch's membrane explants were debrided to the level of the ICL, and those explants receiving BCE cells were cultured for 14 days, to allow maximum ECM deposition.

Fetal Cell Preparation

After removal of muscle and conjunctiva from the exterior of the globe, fetal eyes (obtained from Advance Bioscience Resources, Inc. Alameda, CA), were dipped briefly in a dilute povidone iodine solution (1:10 dilution) and rinsed briefly with DMEM supplemented with 2.5 μg/mL amphotericin B. RPE cells were isolated from fetal eyes ($N = 18$; mean age $\pm$ SEM $= 18.25 \pm 0.50$ weeks) after incubation of RPE/choroid pieces in 0.8 mg/mL collagenase type IV (Sigma-Aldrich), as described previously.[48,56,57] RPE cells were cultured in RPE medium on BCE-ECM-coated tissue culture dishes prepared according to a previously described protocol that routinely generates immunohistochemistry-proven RPE cell cultures in our laboratory.[54] After achieving confluence, primary cultures were passaged at a 1:6 ratio onto BCE-ECM-coated dishes, with 0.25% trypsin-EDTA used to harvest the cells. Subsequent cultures were passaged at a 1:4 ratio.

Experimental Design

All eyes were normal with no or a few submacular drusen except for one 1-day macula (80-year-old Caucasian) with intermediate-size drusen with associated RPE hyperplasia and one 21-day explant pair (78-year-old African American) with extensive drusen in both maculae (Table 1). To assess the ability of cells to attach and spread on treated and untreated surfaces, we seeded fetal RPE cells at a low density (885 cells/mm^2) for 1 day. Explants for long-term survival assessment (14 and 21 days after RPE seeding) were seeded at a higher density (3164 cells/mm^2). This density has been shown to yield a monolayer of cells on a 6 mm-diameter Bruch's membrane explant in organ culture 1 day after seeding (Johnson AC, et al. *IOVS* 2008;49:ARVO E-Abstract 3562).[47,48,55] Explants with seeded fetal RPE cells were cultured in RPE medium that was changed three times per week. Three groups of donor maculae were compared at the 21-day organ culture time point: young (donor age, 41–47 years, four Caucasian, one African American), aged African American (donor age, 52–78 years), and aged Caucasian (donor age, 60–85 years). Explants were harvested after 1, 14, or 21 days in organ culture and placed overnight in 2% paraformaldehyde and 2.5% glutaraldehyde before bisection for light (LM) and scanning electron microscopy (SEM).

Analysis

Scanning Electron Microscopy (SEM). Specimens were postfixed in phosphate-buffered osmium tetroxide, dehydrated in a graded series of ethanol, critical-point dried (Tousimis, Rockville, MD), and sputter coated (Denton, Moorestown, NJ) according to standard SEM protocols. Images were acquired by a scanning electron microscope (JSM 6510; JEOL, Tokyo, Japan) with routine photography at 30×, 50×, 200×, and 1000×. SEM evaluation of Bruch's membrane involved assessment of fetal RPE surface morphology, the degree of ECM coverage, and the level of Bruch's membrane exposed by RPE debridement in areas not resurfaced by cells. To quantify surface coverage, 8 to 10 nonoverlapping fields in the central 3-mm diameter of explants were photographed at 200×. Area measurements were performed by using NIH Image J (http://rsb.info.nih.gov/ij/index.html; developed by Wayne Rasband, National Institutes of Health, Bethesda, MD) to outline areas not resurfaced by cells. This area was subtracted from the total area photographed, to obtain area resurfaced and was expressed as a percentage of Bruch's membrane covered by RPE cells.

Light Microscopy (LM). Bruch's membrane explant halves processed for histology were embedded in resin (LR White; Electron Microscopy Supply, Chestnut Hill, MA). Four to six sections of 2-μm thickness were mounted on slides, dried overnight, and stained with 0.03% toluidine blue (Electron Microscopy Supply). LM evaluation focused on RPE morphology (cell shape, density, pigmentation, polarization) and evaluation of Bruch's membrane and choroid. Nuclear density (ND) counts were performed to assess treatment success quantitatively, comparing BCE-treated submacular explants with control submacular explants from fellow eyes. The number of RPE nuclei in intact cells in contact with Bruch's membrane in the central 3 mm of four to five nonconsecutive slides (every fifth slide) were determined.[48] Linear measurements of Bruch's membrane in the analyzed area were obtained by digital image acquisition and measurement with the freehand line tool using NIH Image J. ND was expressed as the number of nuclei per millimeter of Bruch's membrane $\pm$ SEM.

Statistics. Area measurements and NDs were tested for statistically significant differences using parametric or nonparametric comparisons. Within each time point and group, differences in pairs were tested for normal distribution and variance. Parametric testing between pairs within each time point was by paired *t*-tests; nonparametric testing was performed with the Wilcoxon rank sum test. For comparisons between time points and comparison between groups (e.g., young, aged Caucasian, and aged African American), the existence of significant differences was determined by one-way ANOVA (parametric) or ANOVA on ranks (nonparametric). If significance was observed ($P < 0.05$), post hoc pairwise multiple-comparison procedures (Holm-Sidak method) determined the significance of differences between pairs of groups.

Bestrophin and RPE65 mRNA Analysis

Total RNA was extracted from fetal RPE on paired explants ($n = 4$ pairs, including a 66-year-old African American and 81-, 75-, and 76-year-old Caucasian donors) 21 days after seeding by gently brushing the cells off into lysis buffer (Cells to Signal; Ambion, Austin, TX). RT-PCR was performed to generate cDNA (High Capacity cDNA Reverse Transcription Kit; Applied Biosystems, Inc. [ABI], Foster City, CA) according to the manufacturer's instructions. Real-time PCR was performed by using gene expression assay kits (Taqman; ABI) for bestrophin and RPE65 (primers and probes not disclosed by the manufacturer). Ex-

pression of bestrophin and RPE65 was normalized to 18s rRNA expression. The results were expressed relative to levels in the explant from the 66-year-old African American (i.e., the youngest of the four donors) and compared by paired *t*-test. Levels for in situ extramacular RPE harvested from a 6-mm trephined punch from an 81-year-old Caucasian donor and a 21-day fetal RPE cell culture on BCE-ECM were included for comparison.

Mass Spectrometry of BCE-ECM

BCE-ECM was harvested by adding lysis buffer (7 M urea, 2 M thiourea, 4% CHAPS, 0.2% ampholytes [BioLytes 3/10; Bio-Rad, Hercules, CA]r-sqb], 0.5% Triton x-100, and protease inhibitors) to six 100-mm culture dishes resurfaced with BCE-ECM, scraping off the ECM, and sonicating the resulting solution. The mixture was centrifuged, and the supernatant was transferred to a fresh tube. The pellet from this first solubilization step was further dissolved in the same lysis buffer with the addition of 1% NP-40, 1% Triton X-100, and 50 mM triethylammonium bicarbonate (TEAB). Proteins from the supernatant of the first solubilization step and from the solubilized pellet were subjected to analysis separately. One hundred micrograms of the proteins from each fraction were reduced by dithiothreitol (DTT) and alkylated with iodoacetamide followed by trypsin digestion overnight (trypsin to protein ratio was 1:20). The resulting peptides were separated by sequential ion exchange and reversed-phase liquid chromatography. The peptides were sequenced by tandem mass spectrometry techniques by using either matrix-assisted laser desorption/ionization time-of-flight (MALDI TOF/TOF) or electrospray ionization (ESI) quadrupole time-of-flight (QTOF) mass spectrometry. In brief, the tryptic peptides were separated by strong cation-exchange chromatography (SCX) with a polysulfoethyl A column (4.6 × 200 mm, 5 μm diameter, 300 Å; Poly LC, Columbia, MD) on a perfusion chromatography system (BioCAD; AB Sciex, Foster City, CA). The peptides were eluted with a 40-minute linear gradient from 100% mobile phase A (10 mM KH_2PO_4 and 20% acetonitrile [ACN]) to 50% mobile phase B (600 mM KCl, 10 mM KH_2PO_4, and 20% ACN), followed by a 10-minute linear gradient from 50% to 100% B, at a flow rate of 1 mL/min. Fifteen fractions were collected, and the peptides were cleaned up on C_{18} spin columns (Pierce, Rockford, IL). Desalted peptides were further separated by reversed-phase liquid chromatography (RPLC) with a capillary C_{18} column (0.1 × 150 mm, 3 μm, 100 Å, C_{18}; PepMap; Dionex, Sunnyvale, CA) on an LC system (Ultimate 3000; Dionex) at a flow rate of 200 nL/min. A 70-minute gradient of solvent A (2% ACN, 0.1% trifluoroacetic acid [TFA for MALDI], or 0.1% formic acid [FA, for QTOF]) and solvent B (85% ACN, 0.1% TFA, for MALDI, or 0.1% FA, for QTOF) was used to elute the peptides from the C_{18} column: 0 to 40 minutes, 2% to 22% B; at 65 minutes, to 40% B; and at 80 minutes, to 95% B. For MALDI MS analysis, the RPLC eluent was mixed with a MALDI matrix (5 mg/mL α-cyano-4-hydroxycinnamic acid [CHCA] in 60% ACN, 5 mM ammonium monobasic phosphate and internal calibrators, 50 fmol/μL each of GFP and ACTH 18-39) in a 1:3 ratio and spotted onto a MALDI plate in a 33 × 10 spot array. The peptides were analyzed on an MALDI-TOF/TOF mass analyzer (AB 4800; AB Sciex) in a plate-wide, data-dependent mode, to sequence the top 15 most abundant peptide ions in each MS spectrum. For LC-MS/MS analysis on QTOF, the RPLC eluent was directly introduced into a nano-ESI source on a QTOF tandem MS system (API-US; Waters Corp. Milford, MA), and the top three most abundant peptides were sequenced in a data-dependent mode. Protein identification was performed by searching the peak lists generated from MS/MS spectra against the bovine IPI database with a local MASCOT search engine (ver. 2.2) (Matrix Science Inc. Boston, MA). Oxidized methionine, carbamidomethyl modified cysteines were set as variable modifications in the search parameters. Proteins with at least one peptide ≥95% CI value were identified; overall the protein false-discovery rate was less than 1%. DAVID Bioinformatics Resources 6.7 was used to identify functional localization of proteins (http://david.abcc.ncifcrf.gov/ provided in the public domain by the National Institute of Allergy and Infectious Diseases [NIAID], Bethesda, MD). Protein localization was cross referenced, and function was determined by GeneCards version 3 database (http://www.genecards.org/ provided in the public domain by the Weizmann Institute of Science, Rehovot, Israel) or a protein knowledge database (http://www.uniprot.org/ provided in the public domain by the European Molecular Biology Laboratory, Heidelberg, Germany).

Results

Day 1

RPE cells cultured on the BCE-treated ICL showed various degrees of attachment and spreading (Fig. 1). The cells were generally present as confluent monolayers or as confluent patches of variable size, except for one explant in which the resurfacing was limited to small patches of confluent cells and single cells. Cell morphology was variable with most explants

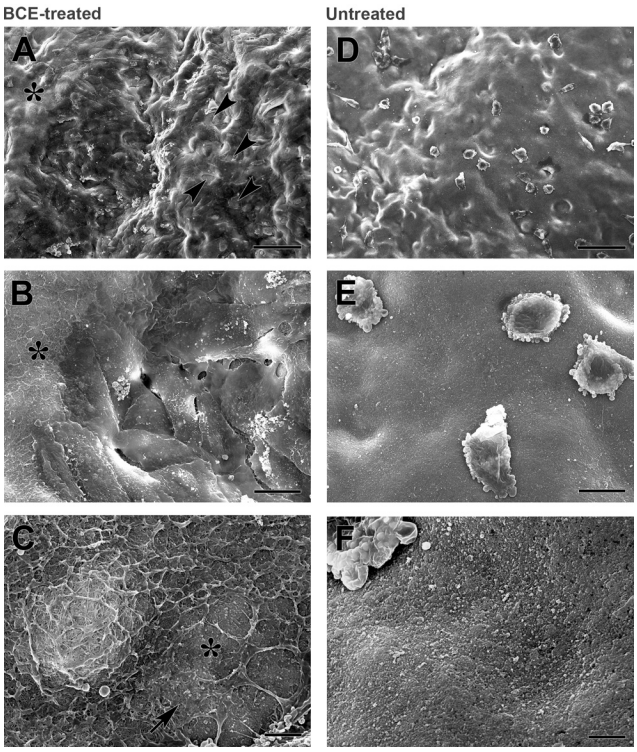

Figure 1. Electron micrographs of fetal RPE resurfacing of submacular Bruch's membrane explants from an 80-year-old Caucasian female donor after 1 day in culture. (**A**) Cells resurfaced the BCE-treated explant as patches of partially confluent cells, creating areas covered by a monolayer of very flat cells. (✻) Unresurfaced area. *Arrowheads*: small defects in the monolayer. ND, 6.54 ± 0.49 nuclei/mm of Bruch's membrane (mean ± SEM). (**B**) Higher magnification of the ICL/cell border of (**A**) (✻ in (**A**) and (**B**) are in the same location in relation to the explant). Cells resurfacing the explant were flat and elongated with no or few apical processes. The meshlike ECM deposition can be seen on the surface of the ICL (✻). (**C**) ECM deposition was highly variable on the BCE-treated explants. In some areas the ECM consisted of a closely knit network of fibers (*arrow*); in other areas, the ECM was sparse with large holes in the network. In some areas, the fibers of the ICL were clearly visible, whereas in other areas the surface of the ICL fibers was covered by a thick layer of deposits (✻). (**D**) Mostly single cells of limited spreading are sparsely present on the untreated explant. ND, 1.86 ± 0.22 nuclei/mm of Bruch's membrane (mean ± SEM). (**E**) Higher SEM magnification of (**D**). Cells on the ICL showed small blebs along their borders. (**F**) The meshlike ECM seen in the BCE-treated explant was not present on the untreated ICL. The surface of the ICL was covered by deposits obscuring a view of most of the collagen fibers. Scale bar: (**A**, **D**) 100 μm; (**B**, **E**) 20 μm; (**C**, **F**) 5 μm.

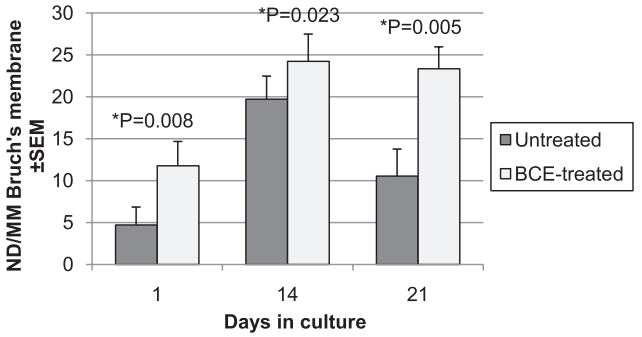

FIGURE 2. ND of fetal RPE on Bruch's membrane from aged Caucasian donor eyes after 1, 14, and 21 days in organ culture. Seeding density for day 1 was 885 cells/mm^2; at days 14 and 21, it was 3164 cells/mm^2. RPE ND was significantly higher on the BCE-treated Bruch's membrane at all time points studied compared with ND on the untreated Bruch's membrane (day 1, $P = 0.008$; day 14, $P = 0.023$; day 21, $P = 0.005$, paired *t*-tests). The NDs on days 14 and 21 were not significantly different (untreated $P = 0.059$; Mann-Whitney rank sum test; BCE-treated $P = 0.633$, unpaired *t*-test).

covered by large, thin, flattened or elongated cells. In areas not resurfaced by cells, the BCE-treated ICL was variably resurfaced by ECM ranging from no visible ECM (as detected by SEM) to a thick, meshlike covering (Fig. 1C). Apoptotic nuclei were observed in four of the seven treated explants. Of the control explants (no exposure to BCE), three explants had no cells or a few poorly spread single cells (Fig. 1). Three explants were resurfaced by single cells and patches of cells similar in morphology to those on BCE-ECM-coated explants, and one explant was partially confluent. In both the BCE-treated and untreated controls, the explants with poor resurfacing by cells showed limited cell spreading, and single cells were commonly present. The morphology of basal linear deposit ranged from fairly lightly staining deposits extending to the outer collagenous layer to heavily stained deposits extending past the intercapillary pillars. The extent of basal linear deposit did not appear to affect RPE cell attachment on the BCE-treated or untreated explants.

The ND of intact RPE on the BCE-treated submacular Bruch's membrane was 11.78 cells/mm of Bruch's membrane ± 2.89 (mean ± SEM; range, 2.27–25.3). The ND of intact RPE on control submacular Bruch's membrane was 4.70 ± 2.14 (range, 0–16.5). The difference was statistically significant (paired *t*-test, $P = 0.008$; Fig. 2).

SEM revealed that flattened cells covered more than 50% of submacular Bruch's membrane ICL in five of seven BCE-treated explants, whereas only one of seven untreated explants showed more than 50% coverage of the ICL. Fetal RPE coverage of the BCE-treated submacular explants ranged from 27.6% to 95% (mean percentage coverage ± SEM = 65.3% ± 0.10%). Cells seeded onto control explants showed resurfacing of submacular ICL ranging from 0.8% to 96% (mean percentage coverage ± SEM, 31.3% ± 0.13%). Bruch's membrane resurfacing by fetal RPE on the BCE-treated explants was significantly greater than resurfacing on control explants ($P = 0.037$, paired *t*-test; Fig. 3). The donor eyes studied at this time point with submacular disease (drusen and focal RPE hyperpigmentation) did not show impairment of attachment and spreading on the BCE-treated (82.0% resurfacing) or on the untreated explant (27.6% resurfacing) compared with BCE-treated and untreated explants without submacular disease.

Day 14

Cell morphology at this time point was characterized by cells of highly variable size and shape, regardless of surface treatment. Cells ranged from enlarged, ballooned cells to smaller cells that were very elongated and spindle shaped, or small and slightly rounded (Fig. 4). The majority of the Bruch's membrane explants were covered with a monolayer of RPE with occasional localized bilayering. BCE-treated explants were fully or almost fully resurfaced, whereas defects in cell coverage were more common in untreated explants. Generally, cells on untreated explants exhibited more signs of deterioration with more vacuole formation, apoptotic nuclei (chromatin aggregation), and cells not well attached to Bruch's membrane (Fig. 4E). The presence of apical processes depended on cell size, regardless of treatment. Very large cells exhibited no apical processes whereas relatively smaller cells showed processes along cell borders only. The smallest cells were covered with short apical processes. NDs of RPE in contact with Bruch's membrane on the BCE-treated explants ranged from 9.5 to 34.3 nuclei/mm of Bruch's membrane (mean ± SEM = 24.2 ± 3.3). NDs of RPE on untreated explants ranged from 6.8 to 27.6 nuclei/mm of Bruch's membrane (mean ± SEM = 19.7 ± 2.8). The ND counts of fetal RPE on explants at day 14 were significantly higher on the BCE-treated explants compared with the untreated explants (paired *t*-test, $P = 0.023$; Fig. 2).

Day 21

Caucasian Donor Bruch's Membrane Explant Resurfacing. Among the BCE-treated explants, 10 of 11 were fully or almost fully resurfaced by fetal RPE (Fig. 5). NDs ranged from 9.48 to 41.3 nuclei/mm of Bruch's membrane (mean ± SEM = 23.4 ± 2.6; Fig. 2). On the explant showing the worst resurfacing (78-year-old donor), the cells were large and ballooned. On the remaining BCE-treated explants, morphology varied between explants and often within explants. Cell morphology ranged from flat or elongate cells with smooth surfaces (no apical processes or processes present around cell borders only, Fig. 5B) to small, compact cells with surfaces covered by short apical processes. Cells were generally in a monolayer. Lightly pigmented cells were seen on three of the 11 BCE-treated explants. Among the untreated explants, six of 11 showed impaired resurfacing with either very few single cells (often not intact), clumps of cells, or few cell patches. Of the remaining five explants, two were resurfaced by predominantly large,

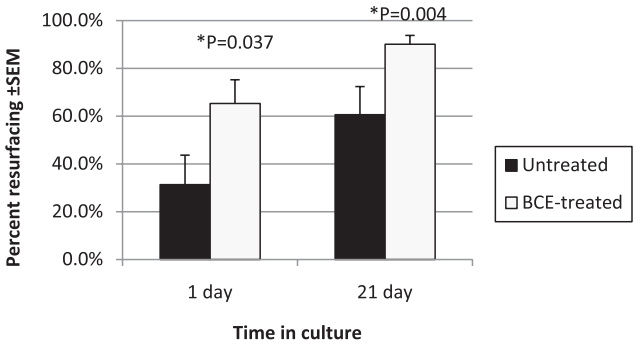

FIGURE 3. Surface coverage of fetal RPE on submacular Bruch's membrane from aged Caucasian donor eyes after 1 and 21 days in organ culture. Fetal RPE cells were seeded at a relatively low seeding density (885 cells/mm^2) for day 1, to observe cell attachment and spreading. Cell resurfacing was significantly higher when seeded onto the BCE-treated ICL than when seeded onto ICL without BCE exposure (untreated; $P = 0.037$, paired *t*-test). Surface coverage of fetal RPE on submacular Bruch's membrane after 21 days in organ culture (seeded at a density of 3164 cells/mm^2) was significantly higher on the BCE-treated ICL than on untreated ICL ($P = 0.004$, Wilcoxon signed rank test). Percentage resurfacing was determined by measuring the area covered by cells in 8 to 10 submacular 200× images acquired by scanning electron microscopy.

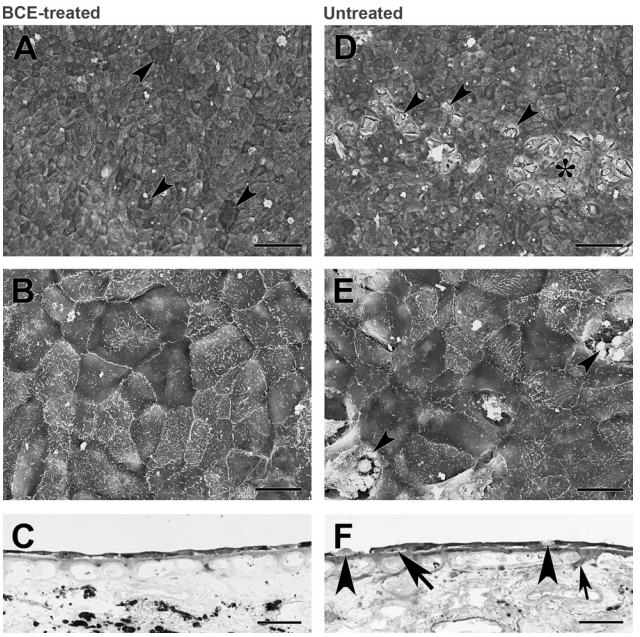

FIGURE 4. Morphology of fetal RPE resurfacing of submacular Bruch's membrane explants from the eyes of a 75-year-old Caucasian woman after 14 days in organ culture. (**A**) Electron micrograph of the BCE-treated explant shows cells resurfaced the explant almost completely as a confluent monolayer. The cells were highly variable in size. *Arrowheads*: very large, flat cells with smooth surfaces. ND, 29.6 ± 0.61 nuclei/mm of Bruch's membrane (mean ± SEM). (**B**) Higher magnification of the cells resurfacing the BCE-treated explant illustrates the variability in cell size and shape. Short apical processes were present on the surface of some cells, whereas others showed little or few apical processes except along their cell borders. (**C**) Light micrograph of BCE-treated explant shows that the cells resurfaced the explant as a monolayer of flattened cells. (**D**) SEM of the untreated explant showed resurfacing similar to that in the fellow explant except for the presence of localized areas of cell death located throughout the submacular surface. *Arrowheads*: small areas where the cells appear to have died; (✻) a larger area of cell death. ND, 23.96 ± 0.41 nuclei/mm of Bruch's membrane (mean ± SEM). (**E**) Higher magnification of the micrograph in (**D**) shows cellular debris in areas of cell death (*arrowheads*). Cells were variable in size and shape, with short apical processes on the surface of some cells. (**F**) Light micrograph of the untreated explant shows the cells were flat and of irregular size and shape. Spindle-shaped cells are common, often with extensions over adjacent cells. *Arrowheads*: cells that are not intact; *large arrow*: a cell filled with vacuoles. Extensive basal linear deposits extend beyond the intercapillary pillars (*small arrow*). (**C**, **F**) Toluidine blue staining. Scale bar: (**A**, **D**) 100 μm; (**B**, **E**) 20 μm; (**C**, **F**) 30 μm.

flat cells; in three explants, defects in RPE cell coverage were more frequent (Fig. 5D). Cell morphology was variable with enlarged, flattened or elongated, smooth, flat cells common (no apical processes) to localized multilayering. Cell pigmentation was observed in some fetal RPE on one untreated explant. Apoptotic nuclei were seen mostly on untreated explants (Fig. 5E). NDs of the untreated explants ranged from 0 to 22.8 nuclei/mm of Bruch's membrane (mean ± SEM = 10.5 ± 3.2; Fig. 2).

All the explants exhibited basal linear deposits in Bruch's membrane, ranging from lightly stained deposits found in the outer collagenous layer to heavily stained deposits extending into and beyond the intercapillary pillars. In general, there did not appear to be a correlation between the amount of basal linear deposit and the degree of RPE resurfacing. Localized areas of choriocapillaris atrophy were present in 4 of 11 BCE-treated explants and in 2 of 11 untreated explants.

The surface area of ICL covered by RPE was significantly higher on the BCE-treated explants than on the untreated explants (Fig. 3, $P = 0.004$, Wilcoxon signed rank test). RPE coverage of the ICL on the BCE-treated explants ranged from 69.1% to 100% (mean ± SEM = 90.1% ± 3.61%). The coverage area on the untreated explants ranged from 0.75% to 99.5% (mean ± SEM = 60.6% ± 11.71%).

RPE cells resurfaced both BCE-treated and untreated ICL of African American explants more uniformly than was observed on the comparable ICL of BCE-treated and untreated Caucasian eyes. Among BCE-treated African-American donor explants, NDs ranged from 24.8 to 34.7 nuclei/millimeter Bruch's membrane (mean ± SEM = 30.1 ± 1.52). Compared with RPE cells on the BCE-treated Caucasian donor explants, cells on African American explants were generally smaller and more uniform in size with apical processes, ranging from processes along cell borders only to surface coverage by moderate-length processes (Fig. 6). Cell morphology was characterized by a mixture of small cells (sometimes elongated) and larger, flat cells. In general, on the untreated explants, the RPE cells were similar to those observed on the BCE-treated explants from the fellow eye but with more defects in coverage. NDs of the untreated explants ranged from 17.7 to 30.4 nuclei/mm of Bruch's membrane (mean ± SEM = 24.1 ± 2.05). Localized areas of multilayering were more common on untreated explants. Light pigmentation was seen in a few RPE cells on one BCE-treated explant.

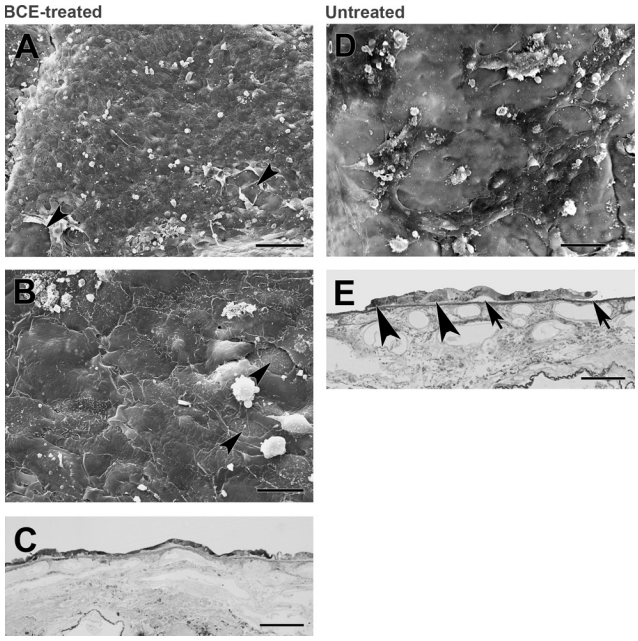

FIGURE 5. Morphology of fetal RPE resurfacing of submacular Bruch's membrane explants from the eyes of a 65-year-old Caucasian male after 21 days in culture. (**A**) Electron micrograph of the BCE-treated explant shows almost complete resurfacing by cells of mixed sizes. *Arrowheads*: defects in cell coverage. ND, 17.43 ± 0.16 nuclei/mm of Bruch's membrane (mean ± SEM). (**B**) Higher magnification of (**A**) shows that the cells are large, flat, and variable in shape. Occasional cells are covered sparsely by short apical processes; many cells have smooth surfaces. *Arrowheads*: small defects in the monolayer. (**C**) Light micrograph of the BCE-treated explant shows the flattened cells with flattened nuclei. (**D**) Electron micrograph of the untreated fellow eye explant shows incomplete resurfacing by patches of large cells. ND, 2.86 ± 0.26 nuclei/mm of Bruch's membrane (mean ± SEM). (**E**) Light micrograph of the untreated explant shows many of the cells were ballooned with enlarged nuclei. *Arrows*: areas where the patch was not well attached. *Arrowheads*: nuclei with clumped chromatin. (**C**, **E**) toluidine blue staining. Scale bar: (**A**, **D**) 100 μm; (**B**) 20 μm; (**C**, **E**) 30 μm.

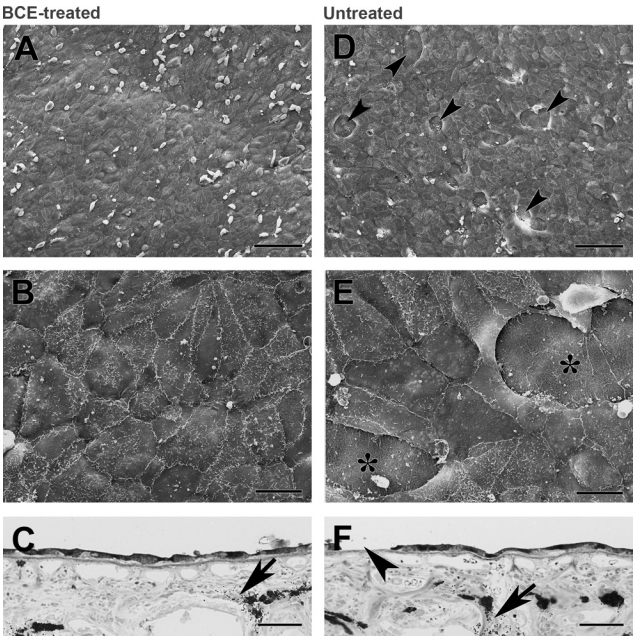

FIGURE 6. Morphology of fetal RPE resurfacing of submacular Bruch's membrane from the eyes of a 52-year-old African American woman after 21 days in culture. (**A**) SEM of the BCE-treated explant shows complete resurfacing by small, flat cells. ND 34.71 ± 0.33 nuclei/mm of Bruch's membrane (mean ± SEM). (**B**) Higher magnification of (**A**). Cells resurfacing the explant were variable in size with prominent apical processes located along the cell borders. Short apical processes are variably present on most of the flattened surfaces of the cells. (**C**) Light micrograph of the BCE-treated explant shows that the cells, although small, were variable in morphology. *Arrow*: an area where pigment granules appear to have been released by adjacent cells. (**D**) SEM of the untreated fellow eye explant shows incomplete resurfacing by cells that are generally larger than those seen on the BCE-treated explant (**A**). *Arrowheads*: some of the small defects in coverage. ND, 31.7 ± 0.36. (**E**) Higher magnification electron micrograph of (**D**) in an area of defects shows the enlarged cells surrounding defects (*asterisks*) in cell coverage. (**F**) Light micrograph of the untreated explant shows flattened cells of variable size resurfacing the explant. *Arrowhead*: a defect in cell coverage; *arrow*: an area of pigment release, presumably from adjacent cells. (**C**, **F**) Toluidine blue staining. Scale bar: (**A**, **D**) 100 μm; (**B**, **E**) 20 μm; (**C**, **F**) 30 μm.

Except for one explant pair (a donor with extensive soft drusen in both maculae), basal linear deposits were generally less in African American explants than in Caucasian donor explants, with some explants showing a thickened elastin layer only and others showing lightly stained deposits extending into the intercapillary pillars. The extensive basal linear deposits in the African American donor with macular soft drusen, which included the formation of basal mounds,[58] did not appear to affect RPE survival in either explant (ND, 33.9 and 30.36 nuclei/mm of Bruch's membrane, for the BCE-treated and the untreated explants, respectively).

Young Donor Bruch's Membrane Explant Resurfacing. NDs of cells on young donor explants ranged from 24.23 to 40.03 nuclei/mm of Bruch's membrane (mean ± SEM = 30.5 ± 2.70) for the BCE-treated explants and 23.90 to 31.75 nuclei/mm of Bruch's membrane (mean ± SEM = 26.1 ± 1.52) for untreated fellow eye explants. Compared with RPE cells on the African American donor explants, cells on the young donor explants appeared to express more differentiated features: more uniformity in size; more closely approximating in situ hexagonal shape; no extremely large, flattened cells; presence of pigmentation; and more apical processes (Fig. 7). On untreated explants, defects in coverage were more likely, and the presence of larger and/or elongated cells was more common. Pigmented cells were more commonly seen in BCE-treated explants than in untreated explants. Basal linear deposits were less than those observed in aged Caucasian donor explants in three of the five donor pairs. In one donor pair (46-year-old), the extent of basal linear deposit was similar to that observed in aged Caucasian donor explants, extending into the intercapillary pillars. Apoptotic nuclei were observed on the untreated explant of this donor. In the second donor pair (45-year-old), extensive choriocapillaris atrophy was seen in the BCE-treated explant. This explant had the highest ND of all those studied (40.03 nuclei/mm of Bruch's membrane) with the cells exhibiting the most differentiated features, including basal location of the nuclei in some but not all cells (Fig. 8). The choriocapillaris and Bruch's membrane were normal in the fellow eye, and basal linear deposit accumulation was pronounced.

ND Analysis at Day 21 in Organ Culture. NDs of the BCE-treated and untreated submacular Bruch's membrane were significantly different between the Caucasian and the African American explants ($P = 0.005$, paired *t*-test; $P = 0.031$ Wilcoxon signed rank test, respectively (Fig. 9), but not between paired explants from young eyes ($P = 0.068$, paired

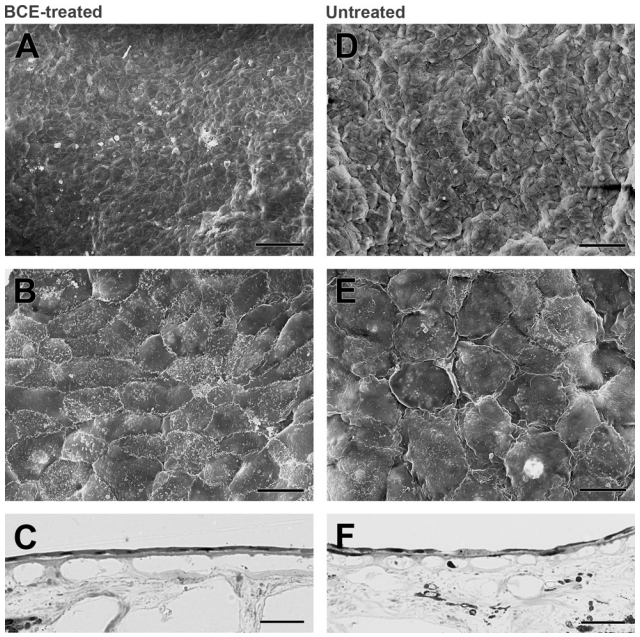

FIGURE 7. Morphology of fetal RPE resurfacing of submacular Bruch's membrane from the eyes of a 45-year-old Caucasian man after 21 days in culture. (**A**) Electron micrograph of the BCE-treated explant shows complete resurfacing by small, flat cells. ND, 34.71 ± 0.33 nuclei/mm of Bruch's membrane ± SEM. (**B**) Higher magnification of (**A**), shows that the cells resurfacing the explant were fairly uniform in size and shape. The small cells had prominent apical processes located along the cell borders, and some cell surfaces were covered by short apical processes. (**C**) Light micrograph of the BCE-treated explant shows a uniform monolayer of flattened cells resurfacing the explant. (**D**) Electron micrograph of the untreated explant shows cells fully resurface the explant, but many of the cells are larger than those resurfacing the BCE-treated explant (**A**). ND, 31.7 ± 0.36. (**E**) Higher magnification of (**D**) shows that the cells were comparatively large with fewer apical processes than on cells resurfacing the BCE-treated explant. Cells on both treated and untreated explants were generally smaller and more uniform than those on the BCE-treated and untreated explants from older Caucasian (Fig. 5) and African American (Fig. 6) donor eyes. (**F**) Light micrograph of the untreated explant shows a monolayer of cells, less uniform in size and shape than that on the fellow explant. (**C**, **F**) Toluidine blue staining. Scale bar: (**A**, **D**) 100 μm; (**B**, **E**) 20 μm; (**C**, **F**) 30 μm.

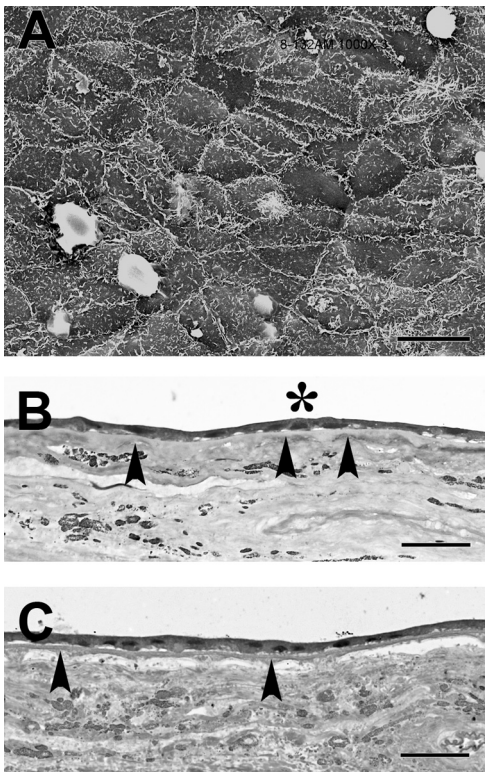

FIGURE 8. Fetal RPE resurfacing of BCE-treated submacular Bruch's membrane from the eye of a 45-year-old Caucasian man with choriocapillaris atrophy. ND, 40.03 ± 0.35 nuclei/mm of Bruch's membrane (mean ± SEM). (**A**) Electron micrograph shows cells completely resurfacing the explant were small with well-developed apical processes along cell borders and on the surface of many of the cells. (**B**) Light micrograph of an area of the explant where there was severe choriocapillaris degeneration and no evident Bruch's membrane sublaminae. *Arrowheads*: degenerated choriocapillaris. Small cells were present on the surface with smallest cells showing basal location of nuclei (three cells under area marked ✻). (**C**) Light micrograph of an adjacent area with choriocapillaris and Bruch's membrane sublaminae (*arrowheads*: the elastic layer). This area of the explant was resurfaced more uniformly with small cells, many showing basal location of nuclei. (**B**, **C**) Toluidine blue staining. Scale bar: (**A**) 20 μm; (**B**, **C**) 30 μm.

t-test). The ages of Caucasian versus African American donors were not significantly different (unpaired *t*-test, $P = 0.054$). One-way ANOVA showed no differences among the NDs of BCE-treated groups ($P = 0.103$), but there was a significant difference in the NDs of untreated groups ($P = 0.003$). All pairwise multiple-comparison testing (Holm-Sidak method) showed significant differences between NDs of the untreated Caucasian and African American donor eyes ($P = 0.005$), and the untreated Caucasian and young eyes ($P = 0.003$), but not between the untreated African American and young eyes ($P = 0.699$). NDs were similar in the BCE-treated Caucasian eyes at 14 and 21 days (24.2 ± 3.26 vs. 21.96 ± 3.12; mean ± SEM, $P = 0.633$ unpaired *t*-test). Although there appeared to be a tendency toward decreased ND from 14 to 21 days in the untreated Caucasian eyes, the decrease was not statistically significant (19.719 ± 2.75 vs. 10.03 ± 3.12; $P = 0.059$, Mann–Whitney rank sum test).

Control Media Studies. Since serum contains ECM ligands that can support cell attachment (e.g., laminin and vitronectin),[59] we performed experiments to determine whether the medium used for culturing BCE cells on explants contributed to the improved RPE resurfacing of BCE-treated Bruch's membrane. Paired submacular explants ($n = 10$, mean age ± SEM, 71.1 ± 2.6 years) were incubated for 2 weeks in ECM medium (includes gentamicin, glutamine, amphotericin, dextran, bFGF, 10% fetal bovine serum, 5% fetal calf serum with 1 ng/mL bFGF added every other day for the first week) or control medium (DMEM supplemented with gentamicin, and amphotericin). The paired explants were treated similarly to the explants cultured with BCE cells (treatment with ammonium hydroxide and washing followed by RPE seeding and culture for 21 days; see the Methods sections). The mean ND, including the two African American explant pairs, in the BCE cell medium was 15.2 ± 2.9 and in the DMEM only was 13.47 ± 3.0; the difference was not significant ($P = 0.315$, paired *t*-test). If the African American explants were excluded (mean African American NDs were 22.3 ± 1.1 in BCE medium, 19.65 ± 6.3 in DMEM, $n = 2$), the mean ND in aged Caucasian eyes ($n = 8$), was 13.4 ± 3.4 in BCE medium versus 11.9 ± 3.4 in DMEM, with no significant differences between pairs, $P = 0.352$ (paired *t*-test). The NDs of RPE in the Caucasian eyes in the control medium studies (13.4 ± 3.4 in BCE cells media vs. 11.9 ± 3.4 in DMEM) were not significantly different from each other (unpaired *t*-test) and were not significantly different from the NDs of cells (10.5 ± 3.2) on the untreated control Caucasian donor explants cultured in DMEM for the same period (Fig. 2; Kruskal-Wallis one-way ANOVA on ranks; $P = 0.788$).

Bruch's Membrane Explant Morphology at Day 1 versus Day 21. The morphology of the Caucasian explants at day 21 was similar to that observed at day 1. Generally, Bruch's membrane and the underlying choroid adjacent to Bruch's membrane were intact. The choriocapillaris endothelial cells were lost in all explants (most likely due to the ammonium hydroxide lysing step to remove BCE). Fiber disruption in the choroid was limited to localized areas and not seen in all explants. Intact pigmented choroidal cells were present in all explants. Pigment release was observed in the choroid of some explants and was most extensive in some but not all of the African American explants (see Fig. 7).

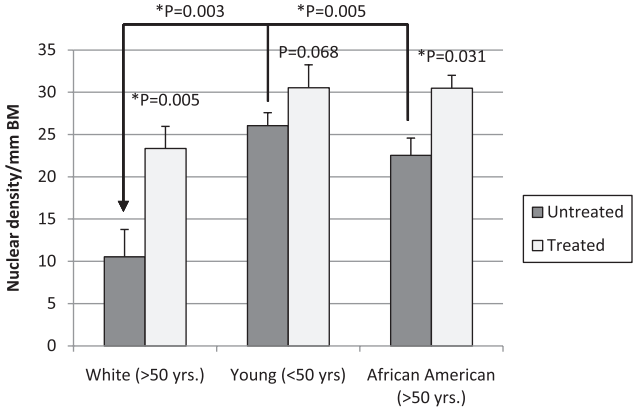

FIGURE 9. ND on submacular ICL of Caucasian and African American donor eyes >50 years of age and young donor eyes <50 (including one African American donor). NDs were compared after seeding of fetal RPE (seeding density, 3164 cells/mm^2) on the BCE-treated and untreated Bruch's membrane explants at day 21 in organ culture. Differences in NDs between BCE-treated and untreated paired explants were significant for Caucasian ICL (White; $P = 0.005$, paired *t*-test) and African American ICL (African American, $P = 0.031$, Wilcoxon signed rank test), but not for young ICL ($P = 0.068$; paired *t*-test). Significant differences were also observed between NDs of untreated Caucasian and young donor explants ($P = 0.003$) and untreated Caucasian and African American explants ($P = 0.005$; one-way ANOVA, all pairwise multiple comparison).

Bestrophin and RPE65 mRNA Expression at Day 21. Messenger RNA expression of bestrophin and RPE65 from fetal RPE harvested from the BCE-treated and untreated explants at day 21 ($n = 4$ donor pairs), from fetal RPE cultured on BCE-ECM-coated tissue culture dishes at day 21, and from in situ RPE from an 81-year-old donor was determined by real time PCR. Results were expressed relative to the BCE-treated explant from a 66-year-old African American donor (Table 2). RPE65 was detected only in in situ RPE and in RPE cells cultured on BCE-ECM-coated tissue culture dishes. Bestrophin was found at low levels in all RPE from the BCE-treated explants (compared with in situ RPE and RPE from culture dishes) and in RPE from two of the four untreated explants. The differences were not statistically significant (paired *t*-test, $P = 0.754$).

Mass Spectrometry of BCE-ECM Harvested from Tissue Culture Dishes. BCE-ECM was difficult to fully solubilize, requiring an additional step to solubilize the pellet resulting from the first solubilization step (see the Methods section). The proteins identified in both fractions (supernatant from the first solubilization step and the solubilized pellet from the second solubilization step) are combined and are presented in Supplementary Table S1, http://www.iovs.org/lookup/suppl/doi:10.1167/iovs.10-6112/-/DCSupplemental. Table 3 lists the identified ECM and ECM-associated proteins (excluding proteins involved in ECM assembly and remodeling) and secreted proteins with functions relating to cell adhesion, migration, proliferation, and survival.

Discussion

The results of previous studies, in which a human Bruch's membrane organ culture bioassay was used that mimics the surface on which RPE must survive in aged human eyes, predicted the poor survival of transplanted cells that has generally been observed in AMD patients undergoing RPE transplantation.[47,48,57,60] The impaired resurfacing appears to occur regardless of the cell type or preparation used (e.g., cultured fetal RPE,[48] freshly harvested adult RPE,[47] cultured adult RPE,[48,56] fresh and cultured adult iris pigment epithelium,[60] and RPE derived from human embryonic stem cells [Johnson AC, et al. *IOVS* 2008;49:ARVO E-Abstract 3562]) or the surface on which the transplanted cells are seeded (e.g., RPE basement membrane, superficial or deep ICL).[48] Cultured human RPE cells express the integrins needed to attach to ECM proteins likely to be found in Bruch's membrane (Sun Q, et al. *IOVS* 2008;49:ARVO E-Abstract 3564)[61] and can, by day 1 after seeding, resurface aged submacular human Bruch's membrane to a similar degree as RPE on BCE-ECM-coated tissue culture dishes, indicating that poor long-term cell survival is not related to the inability of cells to attach to Bruch's membrane.[48] Survival of RPE on aged submacular human Bruch's membrane appears to decrease with time in culture[48] and may depend on age-related changes in Bruch's membrane, as indicated by the results presented herein (Fig. 9). RPE NDs at day 21 in organ culture demonstrated a further decline in cell survival compared to that observed in our previously published study showing a decline in RPE ND from day 1 to day 14.[48] With normal aging, human Bruch's membrane, especially in the submacular region, undergoes numerous changes (e.g., increased thickness, deposition of lipids, cross-linking of proteins, and nonenzymatic formation of advanced glycation end products).[35,49] These changes and additional changes due to AMD could decrease the bioavailability of ECM proteins (e.g., laminin, fibronectin, collagen IV, proteoglycans, growth factors), limiting supportive cell–matrix interactions and leading to poor survival and differentiation of transplanted RPE cells in eyes with AMD. Because the changes in Bruch's membrane from aging and AMD are complex and may not be fully reversible, one approach to improve RPE transplant success is to establish a new ECM over Bruch's membrane.

The goal of these experiments was not to identify a surgical technique for RPE transplantation in humans. Our goal was to determine whether providing a provisional ECM can favorably influence RPE survival on aged and AMD submacular human Bruch's membrane. The data seem to indicate that it is possible to do so. The use of ICL (vs. basement membrane) as the recipient bed was simply a strategy to improve BCE cell attachment to and growth on aged/AMD submacular Bruch's membrane, so that BCE-ECM could be deposited in significant amounts. (BCE cell growth and ECM deposition on ICL is greater than on aged submacular human RPE basement membrane.) The approach that one might take to translate these findings into clinical practice probably would depend on identifying the essential components of BCE-ECM that mediate this beneficial effect. Once those components are identified, there are several ways in which they may be introduced into the subretinal space (e.g., via a nanoengineered scaffold decorated with the components with or without attached RPE, via a soluble mixture of essential components). Removal of native RPE basement membrane, should it be necessary, can be achieved with gentle mechanical debridement, as is done in the laboratory and as we have done in vivo previously.[62]

Although the extent of ECM deposition on the BCE-treated Bruch's membrane explants is not known, the results indicate that, to some degree, BCE cells can deposit BCE-ECM on aged human submacular Bruch's membrane (Fig. 1) and that fetal RPE survival is improved as a result. Because of the inability of aged submacular Bruch's membrane to support cell survival generally, BCE-ECM deposition was highly variable and did not appear to be deposited to the same degree as is seen on tissue culture dishes. The effect of the underlying substrate on ECM deposition was demonstrated by the fact that BCE cells were able to deposit ECM on the ICL to a greater degree than on RPE basement membrane from aged eyes. Since the ECM components deposited can vary depending on the substrate to which the cells are attached,[63] different degrees of aging changes in the ICL could lead to variable ECM component deposition, which could be a confounding factor between donors and in localized areas of the same donor explant that show poor resurfacing despite SEM evidence of ECM deposition. The rel-

Table 2. Messenger RNA Bestrophin and RPE65 Expression of Fetal RPE after 21 Days in Culture on BCE-Treated and Untreated Bruch's Membrane Explants

Donor	Surface Treatment	Bestrophin	RPE65
66AAF	BCE-treated	1	ND
	Untreated	0	ND
81CF	BCE-treated	0.43	ND
	Untreated	0	ND
75CM	BCE-treated	3.91	ND
	Untreated	0.17	ND
76CF	BCE-treated	8.57	ND
	Untreated	0.48	ND
81CF	In situ	70.8	366.8
21-day RPE culture	BCE-ECM on culture dish	133.8	18.7

Expression is relative to bestrophin expression in the youngest donor (66-year-old African American woman). Bestrophin and RPE65 mRNA expression from in situ RPE from an 81-year-old donor and from a 21-day fetal RPE culture are included for comparison. RPE65 expression was not detected (ND) in fetal RPE cultured on BCE-treated and untreated explants. Bestrophin levels were not significantly different in RPE derived from BCE- treated vs. untreated explants ($P = 0.754$). AAF, African American female; CF, Caucasian female; CM, Caucasian male.

TABLE 3. Proteins Identified in BCE-ECM Harvested from Tissue Culture Dishes

Accession Number	Protein Name	Protein Molecular Weight
ECM and ECM-Associated Proteins		
IPI00685669	MFAP2 Microfibrillar-associated protein 2	20695
IPI00913833	LOC783816 similar to collagen triple helix repeat containing 1	25703
IPI00698668	CTGF Connective tissue growth factor	37898
IPI00716158	LUM Lumican	38732
IPI00815631	LOC534844 similar to thrombospondin type-1 domain-containing protein 4	41545
IPI00710385	PRELP Prolargin (proline/arginine-rich end leucine-rich repeat protein)	43655
IPI00824488	COL4A4 Collagen alpha-4(IV) chain (fragment)	46355
IPI00685697	EFEMP2 EGF-containing fibulin-like extracellular matrix protein 2	49650
IPI00686824	TGFB3 TGFB3 protein (transforming growth factor, beta 3)	51287
IPI00712934	VTN Vitronectin	53541
IPI00696930	EFEMP1 EGF-containing fibulin-like extracellular matrix protein 1	55044
IPI00906639	ECM1 60 kDa protein	60357
IPI00697984	NTN4 NTN4 protein (netrin 4)	69928
IPI00826312	NPNT similar to nephronectin precursor	71203
IPI00685504	COL8A1 Alpha 1 type VIII collagen (fragment)	73198
IPI00709922	FBLN1 FBLN1 protein (fibulin 1)	77715
IPI00690783	POSTN Periostin, osteoblast specific factor	86804
IPI00707932	COL8A2 collagen, type VIII, alpha 2	90571
IPI00692544	EMILIN 1 similar to EMILIN-1 precursor (elastin microfibril interface located protein)	106822
IPI00717179	CCDC80 CCDC80 protein (coiled-coil domain containing 80)	108157
IPI00708244	COL1A2 Collagen alpha-2(I) chain	128985
IPI00696401	THBS1 Thrombospondin-1	129392
IPI00712084	THBS1 Thrombospondin-1	129451
IPI00688802	NID1 NID1 protein (nidogen 1)	136353
IPI00731432	COL3A1 Collagen, type III, alpha 1	138354
IPI00867435	NID2 NID2 protein (nidogen 2)	142578
IPI00698002	LAMC1 similar to laminin subunit gamma-1 precursor	143111
IPI00905162	NID2 151 kDa protein	151065
IPI00729819	COL4A5 similar to alpha 5 type IV collagen isoform 2	158575
IPI00706758	COL16A1 similar to alpha 1 type XVI collagen	158944
IPI00687437	COL4A1 Collagen, type IV, alpha 1	160330
IPI00709244	COL4A3 Collagen, type IV, alpha 3	160501
IPI00912158	COL4A5 similar to alpha 5 type IV collagen isoform 1	161767
IPI00712524	COL4A2 Collagen, type IV, alpha 2, partial	164404
IPI00698418	LAMC3 similar to laminin, gamma 3	171371
IPI00824553	COL11A1 Collagen, type XI, alpha 1 isoform 4	176527
IPI00727431	TNC Tenascin C	190961
IPI00904771	LAMC1 Laminin, beta 2	196079
IPI00690076	LAMB1 Laminin B1 protein	197339
IPI00686590	LOC100138045 similar to laminin alpha 3 subunit	229860
IPI00728194	FN1 fibronectin 1 isoform 12	259593
IPI00714673	FN1 Embryo-specific fibronectin 1 transcript variant	262263
IPI00728875	FN1 Fibronectin	272154
IPI00711115	FBN1 Fibrillin-1	312036
IPI00714359	FBN1 313 kDa protein (fibrillin 1)	312390
IPI00709514	FBN3 similar to fibrillin3	327863
IPI00729261	COL12A1 Collagen, type XII, alpha 1 isoform 1	351047
IPI00717460	LAMA5 similar to laminin, alpha 5	370801
IPI00713324	TNXB Tenascin-X	447103
IPI00712795	HSPG2 heparan sulfate proteoglycan 2	467733
Secreted Non-ECM Proteins		
IPI00839037	PF4 13 kDa protein (platelet factor 4)	12567
IPI00867416	PF4 PF4 protein (platelet factor 4)	12601
IPI00702598	WNT5A similar to Wnt-5a isoform 1	42292
IPI00715866	TGFB2 Transforming growth factor beta-2	47748
IPI00715339	FBLN5 Fibulin-5	50131
IPI00711678	ANGPTL2 Angiopoietin-like protein 2	56947
IPI00694104	PLAT Tissue-type plasminogen activator	63659
IPI00715828	C6H4ORF31 Chromosome 4 open reading frame 31 ortholog (fibronectin type-III domain-containing protein C4orf31 precursor)	64389
IPI00905771	QSOX1 73 kDa protein	73054
IPI00867404	ADAMTSL4 ADAMTSL4 protein (ADAMTS-like protein 4 precursor)	116226
IPI00730859	LTBP3 similar to latent transforming growth factor beta binding protein 3	138457
IPI00718698	LTBP2 latent transforming growth factor beta binding protein 2	211448

Proteins (selected from Supplementary Table S1, http://www.iovs.org/lookup/suppl/doi:10.1167/iovs.10–6112/-/DC1) that are ECM proteins and/or secreted proteins with functions related to cell adhesion, proliferation, apoptosis, and differentiation are shown.

ative lack of expression of differentiation markers in RPE grown on BCE-ECM-coated submacular Bruch's membrane may be due to reduced ECM deposition on aged human Bruch's membrane compared with the extent of ECM deposition that occurs when these same cells are grown on BCE-ECM-coated tissue culture dishes. Nonetheless, RPE attachment, resurfacing, morphology, and ND were all superior after ECM-coating of aged submacular human Bruch's membrane compared with uncoated fellow eyes. It is possible that if a BCE-ECM coating could be applied uniformly to aged Bruch's membrane as it is in tissue culture dishes, then RPE survival and differentiation would be better than we observed. The effect of the Bruch's membrane race and age on the ability of RPE to differentiate and express bestrophin and RPE-65 could not be determined because of the scarcity of tissue from young and African American donors.

The degree of improvement in cell survival on aged Bruch's membrane observed in this study is significantly more than has been reported previously. Adding exogenous individual ECM ligands (e.g., combinations of laminin, fibronectin, vitronectin, and collagen IV) improved initial adult RPE attachment to aged peripheral Bruch's membrane to a limited degree.[51] Treating ICL from peripheral areas with Triton to extract the abnormal deposits before coating with ECM ligands is reported to result in better RPE survival, but our interpretation of the published micrographs is that the cells tend to have abnormal morphology and limited (~21%) coverage, which correlates with a very low ND.[52] The surface coverage in the Triton-treatment study was approximately one third that observed on our untreated explants at day 21 (60.6%). Although it is not clear whether cell behavior on peripheral ICL is similar to that of submacular ICL, differences other than the method of Bruch's membrane treatment also may have contributed to the higher survival in our study: the RPE seeding density for long-term studies was much higher in the present study (3164 vs. 531 cells/mm^2); our untreated explants were soaked for 14 days in DMEM before seeding fetal RPE; the differences in fetal RPE culture before seeding on Bruch's membrane (i.e., difference in passage number and time in culture before harvest) may be important; and the RPE cells that we used were harvested from ECM-coated dishes and seeded on ECM-coated Bruch's membrane, which renders the ECM on Bruch's membrane similar to that on which the cells were cultured before harvest.

We recognize that many different cell types may be transplanted with benefit in AMD eyes, including human embryonic stem cell–derived RPE (hES-RPE), virally transformed RPE, and non-RPE cells.[5,14,17,64–69] However, fetal RPE cells were used for these experiments because this study required a large number of cells for organ culture assays. Primary and early passage fetal RPE cultures grow rapidly, and cultures of early passage cells (passages 1–4), used within 2 to 6 days of seeding, were seeded on explants to allow consistency in cells between experiments since higher passage cells grow slowly, and cells that have been in culture for long periods of time take longer to recover from harvest. To preserve the robustness of the cells, fresh (not frozen) cells were used to allow for attachment assessment at 1 day after seeding. Since BCE-ECM supports a variety of cell types, we suspect the improved resurfacing and survival shown here with fetal RPE would also apply to other cells that could be considered for cell transplantation (e.g., adult RPE, IPE, and hES-RPE).

Although this study illustrates an approach to improve RPE transplant survival on aged human Bruch's membrane, the technique used to provide the new ECM could not be applied in patients. We hypothesize that if a three-dimensional matrix similar to BCE-ECM can be applied to submacular Bruch's membrane surgically (rather than relying on cell synthesis in situ), then uniform resurfacing of submacular Bruch's membrane by transplanted RPE can be achieved. Currently, we believe that solubilization of BCE-ECM as an approach to coating Bruch's membrane is not feasible because harsh methods are necessary to solubilize the ECM components. The complexity of BCE-ECM composition, as indicated by the extensive list of proteins found by mass spectrometry, renders identification of the active, cell-supporting components in the ECM a daunting challenge. In addition to ECM and ECM-associated proteins, other proteins (typically localized to the cell membrane and intracellularly) were identified in the ECM protein analysis. This finding may indicate that despite the protocols used to remove BCE cells from Bruch's membrane after ECM deposition, remnants of BCE cells may persist on Bruch's membrane. The influence of these intracellular protein components on RPE cell attachment to and/or survival on aged Bruch's membrane is unknown.

Campochiaro and Hackett[70] showed more rapid RPE differentiation on ECM deposited by BCE cells after 1 week in culture than on ECM deposited by RPE cells after 1 week in culture. It is not clear from these studies whether the difference in RPE differentiation on BCE-ECM$_{1\ week}$ vs. RPE-ECM$_{1\ week}$ reflects differences in RPE versus BCE-ECM composition and/or differences in the amount of ECM deposition. (RPE-ECM deposition is slower than BCE-ECM deposition.[70]) Mass spectroscopy analysis showed that BCE-ECM contains components that have also been identified in RPE-ECM (e.g., laminin, fibronectin, and collagens I, III, and IV).[71–73] Basic fibroblast growth factor (bFGF), which is found in both RPE-ECM and BCE-ECM,[70,74] was not detected in BCE-ECM in our studies, possibly due to low levels. RPE can secrete proteoglycans (e.g., heparan sulfate proteoglycan, lumican, and biglycan) and ECM glycoproteins (e.g., precursors or subunits of collagens II, V, VI, XI, XII, and XV; nidogen; and vitronectin) although these components have not been identified in RPE-ECM as far as we know.[75,76] Among collagens I and IV in RPE-ECM, collagen IV appears to be the most abundant,[77] while collagen III is the most abundant collagen in BCE-ECM, accounting for 60% or more of the total collagen content.[78,79] Collagen III is a fibrillar collagen; fibrillar collagens can regulate cell adhesion, proliferation, and differentiation.[80] Collagen VIII, a network-forming collagen not specifically identified in RPE-ECM or secreted by RPE, forms the hexagonal lattice structures of BCE-ECM.[81] Both collagen III and VIII are found in human Descemet membrane,[82] a substrate that supports both IPE and RPE in culture.[83] BCE-ECM also contains collagen XVI, a collagen not identified in secretion profiles of RPE. Collagen XVI is a member of the FACIT collagen family (fibril-associated collagens with interrupted helices) and is thought to attach to fibrillar collagen, functioning in maintaining the integrity of the ECM.[84] Thus, the collagens in BCE-ECM that are not associated with RPE secretion and possibly are not present in RPE-ECM appear to be proteins with the potential to regulate cell behavior and may contribute to differences in RPE behavior on BCE-ECM versus RPE-ECM.

The composition analyses in this study were performed on BCE-ECM deposited on culture dishes. We do not know the composition of BCE-ECM on Bruch's membrane. Our observations show that, for a given time in culture, BCE-ECM deposition is less on aged submacular human Bruch's membrane than on tissue culture plastic. The ECM deposited on Bruch's membrane was morphologically similar to that found by Sawada et al.[85] in early BCE cells cultures (up to 10 days). Nevertheless, even with the lesser amount of ECM deposition, BCE-ECM deposition on aged/AMD submacular human Bruch's membrane is associated with significant improvement in RPE survival compared with that in untreated controls.

The results suggest that submacular ICL from Caucasian patients over 50 years of age will benefit the most from treatment of Bruch's membrane, as RPE cell survival on this surface was significantly more impaired than on African American and young ICL. Caucasians are more likely than African Americans

to develop late-stage AMD,[86–91] and, therefore, are more likely to need treatment. It is not clear whether the factors that render African Americans relatively resistant to the late complications of AMD also are responsible for the improved RPE survival on aged submacular Bruch's membrane (compared to Caucasian donors) that we observed. The high variability in the NDs of untreated and treated Caucasian donor eyes, especially when compared with that of African American and young donor eyes, may very well be a reflection of the highly variable degree of AMD changes found in this population. The sample size for African American and young donor eyes was relatively small, and it is possible that differences in attachment, spreading, and proliferation compared to Caucasian donor eyes may be due to sampling error. However, there was relatively little variability in the data from the African American and young donor cohorts. The number of African American eyes used in this study was relatively small due to the scarcity of such donor tissue meeting our acceptance criteria. Thus, the degree to which this group would benefit from ECM treatment of Bruch's membrane at the time of RPE transplantation is not clear.

In conclusion, we have shown that RPE transplant survival in human submacular Bruch's membrane organ culture can be improved significantly by coating Bruch's membrane with cell-deposited ECM and that this treatment is effective for cell transplantation onto Bruch's membrane over age 50 years. The results indicate that, if a method of coating aged/diseased Bruch's membrane with an ECM similar to that secreted by BCE cells can be devised, the success of RPE transplantation will improve.

Acknowledgments

The authors thank Carola Springer for technical assistance.

References

1. Friedman DS, O'Colmain BJ, Munoz B, et al. Prevalence of age-related macular degeneration in the United States. *Arch Ophthalmol.* 2004;122:564–572.
2. Brown DM, Kaiser PK, Michels M, et al. Ranibizumab versus verteporfin for neovascular age-related macular degeneration. *N Engl J Med.* 2006;355:1432–1444.
3. Rosenfeld PJ, Brown DM, Heier JS, et al. Ranibizumab for neovascular age-related macular degeneration. *N Engl J Med.* 2006;355:1419–1431.
4. A randomized, placebo-controlled, clinical trial of high-dose supplementation with vitamins C and E, beta carotene, and zinc for age-related macular degeneration and vision loss: AREDS report no. 8. *Arch Ophthalmol.* 2001;119:1417–1436.
5. Kanuga N, Winton HL, Beauchene L, et al. Characterization of genetically modified human retinal pigment epithelial cells developed for in vitro and transplantation studies. *Invest Ophthalmol Vis Sci.* 2002;43:546–555.
6. Becerra SP, Fariss RN, Wu YQ, Montuenga LM, Wong P, Pfeffer BA. Pigment epithelium-derived factor in the monkey retinal pigment epithelium and interphotoreceptor matrix: apical secretion and distribution. *Exp Eye Res.* 2004;78:223–234.
7. Marneros AG, Fan J, Yokoyama Y, et al. Vascular endothelial growth factor expression in the retinal pigment epithelium is essential for choriocapillaris development and visual function. *Am J Pathol.* 2005;167:1451–1459.
8. Bost LM, Aotaki-Keen A, Hjelmeland LM. Coexpression of FGF5 and bFGF by the retinal pigment epithelium in vitro. *Exp Eye Res.* 1992;55:727–734.
9. Hackett SF, Schoenfeld CL, Freund J, Gottsch JD, Bhargave S, Campochiaro PA. Neurotrophic factors, cytokines and stress increase expression of basic fibroblast growth factor in retinal pigmented epithelial cells. *Exp Eye Res.* 1997;64:865–874.
10. Faktorovich EG, Steinberg RH, Yasumura D, Matthes MT, LaVail MM. Photoreceptor degeneration in inherited retinal dystrophy delayed by basic fibroblast growth factor. *Nature.* 1990;347:83–86.
11. Martin G, Schlunck G, Hansen LL, Agostini HT. Differential expression of angioregulatory factors in normal and CNV-derived human retinal pigment epithelium. *Graefes Arch Clin Exp Ophthalmol.* 2004;242:321–326.
12. Gullapalli VK, Khodair M, Wang H, Sugino IK, Madreperla S, Zarbin MA. Retinal pigment epithelium and photoreceptor transplantation frontiers. In: Ryan SJ, ed. *Retina*. 4th ed. Philadelphia: Elsevier Mosby, Inc.; 2006:2597–2613.
13. Li L, Turner JE. Optimal conditions for long-term photoreceptor cell rescue in RCS rats: the necessity for healthy RPE transplants. *Exp Eye Res.* 1991;52:669–679.
14. Coffey PJ, Girman S, Wang SM, et al. Long-term preservation of cortically dependent visual function in RCS rats by transplantation. *Nat Neurosci.* 2002;5:53–56.
15. Gouras P, Kong J, Tsang SH. Retinal degeneration and RPE transplantation in Rpe65(−/−) mice. *Invest Ophthalmol Vis Sci.* 2002;43:3307–3311.
16. Wang NK, Tosi J, Kasanuki JM, et al. Transplantation of reprogrammed embryonic stem cells improves visual function in a mouse model for retinitis pigmentosa. *Transplantation.* 2010;89:911–919.
17. Lu B, Malcuit C, Wang S, et al. Long-term safety and function of RPE from human embryonic stem cells in preclinical models of macular degeneration. *Stem Cells.* 2009;27:2126–2135.
18. Nozaki M, Raisler BJ, Sakurai E, et al. Drusen complement components C3a and C5a promote choroidal neovascularization. *Proc Natl Acad Sci U S A.* 2006;103:2328–2333.
19. Hageman GS, Anderson DH, Johnson LV, et al. A common haplotype in the complement regulatory gene factor H (HF1/CFH) predisposes individuals to age-related macular degeneration. *Proc Natl Acad Sci U S A.* 2005;102:7227–7232.
20. Klein RJ, Zeiss C, Chew EY, et al. Complement factor H polymorphism in age-related macular degeneration. *Science.* 2005;308:385–389.
21. Edwards AO, Ritter R 3rd, Abel KJ, Manning A, Panhuysen C, Farrer LA. Complement factor H polymorphism and age-related macular degeneration. *Science.* 2005;308:421–424.
22. Haines JL, Hauser MA, Schmidt S, et al. Complement factor H variant increases the risk of age-related macular degeneration. *Science.* 2005;308:419–421.
23. Hughes AE, Orr N, Esfandiary H, Diaz-Torres M, Goodship T, Chakravarthy U. A common CFH haplotype, with deletion of CFHR1 and CFHR3, is associated with lower risk of age-related macular degeneration. *Nat Genet.* 2006;38:1173–1177.
24. Skerka C, Lauer N, Weinberger AA, et al. Defective complement control of factor H (Y402H) and FHL-1 in age-related macular degeneration. *Mol Immunol.* 2007;44:3398–3406.
25. Gold B, Merriam JE, Zernant J, et al. Variation in factor B (BF) and complement component 2 (C2) genes is associated with age-related macular degeneration. *Nat Genet.* 2006;38:458–462.
26. Yates JR, Sepp T, Matharu BK, et al. Complement C3 variant and the risk of age-related macular degeneration. *N Engl J Med.* 2007;357:553–561.
27. He X, Hahn P, Iacovelli J, et al. Iron homeostasis and toxicity in retinal degeneration. *Prog Retin Eye Res.* 2007;26:649–673.
28. Dewan A, Liu M, Hartman S, et al. HTRA1 promoter polymorphism in wet age-related macular degeneration. *Science.* 2006;314:989–992.
29. Rivera A, Fisher SA, Fritsche LG, et al. Hypothetical LOC387715 is a second major susceptibility gene for age-related macular degeneration, contributing independently of complement factor H to disease risk. *Hum Mol Genet.* 2005;14:3227–3236.
30. Jakobsdottir J, Conley YP, Weeks DE, Mah TS, Ferrell RE, Gorin MB. Susceptibility genes for age-related maculopathy on chromosome 10q26. *Am J Hum Genet.* 2005;77:389–407.
31. Schmidt S, Hauser MA, Scott WK, et al. Cigarette smoking strongly modifies the association of LOC387715 and age-related macular degeneration. *Am J Hum Genet.* 2006;78:852–864.
32. Conley YP, Jakobsdottir J, Mah T, et al. CFH, ELOVL4, PLEKHA1 and LOC387715 genes and susceptibility to age-related maculopathy: AREDS and CHS cohorts and meta-analyses. *Hum Mol Genet.* 2006;15:3206–3218.

33. Shastry BS. Further support for the common variants in complement factor H (Y402H) and LOC387715 (A69S) genes as major risk factors for the exudative age-related macular degeneration. *Ophthalmologica.* 2006;220:291–295.
34. Kanda A, Chen W, Othman M, et al. A variant of mitochondrial protein LOC387715/ARMS2, not HTRA1, is strongly associated with age-related macular degeneration. *Proc Natl Acad Sci U S A.* 2007;104:16227–16232.
35. Zarbin MA. Current concepts in the pathogenesis of age-related macular degeneration. *Arch Ophthalmol.* 2004;122:598–614.
36. Zhou J, Jang YP, Kim SR, Sparrow JR. Complement activation by photooxidation products of A2E, a lipofuscin constituent of the retinal pigment epithelium. *Proc Natl Acad Sci U S A.* 2006;103: 16182–16187.
37. Donoso LA, Kim D, Frost A, Callahan A, Hageman G. The role of inflammation in the pathogenesis of age-related macular degeneration. *Surv Ophthalmol.* 2006;51:137–152.
38. Shen JK, Dong A, Hackett SF, Bell WR, Green WR, Campochiaro PA. Oxidative damage in age-related macular degeneration. *Histol Histopathol.* 2007;22:1301–1308.
39. Li LX, Turner JE. Inherited retinal dystrophy in the RCS rat: prevention of photoreceptor degeneration by pigment epithelial cell transplantation. *Exp Eye Res.* 1988;47:911–917.
40. Pinilla I, Cuenca N, Sauve Y, Wang S, Lund RD. Preservation of outer retina and its synaptic connectivity following subretinal injections of human RPE cells in the Royal College of Surgeons rat. *Exp Eye Res.* 2007;85:381–392.
41. Algvere PV, Gouras P, Dafgard Kopp E. Long-term outcome of RPE allografts in non-immunosuppressed patients with AMD. *Eur J Ophthalmol.* 1999;9:217–230.
42. Binder S, Krebs I, Hilgers RD, et al. Outcome of transplantation of autologous retinal pigment epithelium in age-related macular degeneration: a prospective trial. *Invest Ophthalmol Vis Sci.* 2004; 45:4151–4160.
43. Tezel TH, Del Priore LV, Berger AS, Kaplan HJ. Adult retinal pigment epithelial transplantation in exudative age-related macular degeneration. *Am J Ophthalmol.* 2007;143:584–595.
44. da Cruz L, Chen FK, Ahmado A, Greenwood J, Coffey P. RPE transplantation and its role in retinal disease. *Prog Retin Eye Res.* 2007;26:598–635.
45. Joussen AM, Joeres S, Fawzy N, et al. Autologous translocation of the choroid and retinal pigment epithelium in patients with geographic atrophy. *Ophthalmology.* 2007;114:551–560.
46. Joussen AM, Heussen FM, Joeres S, et al. Autologous translocation of the choroid and retinal pigment epithelium in age-related macular degeneration. *Am J Ophthalmol.* 2006;142:17–30.
47. Tsukahara I, Ninomiya S, Castellarin A, Yagi F, Sugino IK, Zarbin MA. Early attachment of uncultured retinal pigment epithelium from aged donors onto Bruch's membrane explants. *Exp Eye Res.* 2002;74:255–266.
48. Gullapalli VK, Sugino IK, Van Patten Y, Shah S, Zarbin MA. Impaired RPE survival on aged submacular human Bruch's membrane. *Exp Eye Res.* 2005;80:235–248.
49. Booij JC, Baas DC, Beisekeeva J, Gorgels TG, Bergen AA. The dynamic nature of Bruch's membrane. *Prog Retin Eye Res.* 2010; 29:1–18.
50. Pauleikhoff D, Wojteki S, Muller D, Bornfeld N, Heiligenhaus A. Adhesive properties of basal membranes of Bruch's membrane: immunohistochemical studies of age-dependent changes in adhesive molecules and lipid deposits (in German). *Ophthalmologe.* 2000;97:243–250.
51. Del Priore LV, Geng L, Tezel TH, Kaplan HJ. Extracellular matrix ligands promote RPE attachment to inner Bruch's membrane. *Curr Eye Res.* 2002;25:79–89.
52. Tezel TH, Del Priore LV, Kaplan HJ. Reengineering of aged Bruch's membrane to enhance retinal pigment epithelium repopulation. *Invest Ophthalmol Vis Sci.* 2004;45:3337–3348.
53. Wang H, Van Patten Y, Sugino IK, Zarbin MA. Migration and proliferation of retinal pigment epithelium on extracellular matrix ligands. *J Rehabil Res Devel.* 2006;43:713–722.
54. Song MK, Lui GM. Propagation of fetal human RPE cells: preservation of original culture morphology after serial passage. *J Cell Physiol.* 1990;143:196–203.
55. Castellarin AA, Sugino IK, Vargas JA, Parolini B, Lui GM, Zarbin MA. In vitro transplantation of fetal human retinal pigment epithelial cells onto human cadaver Bruch's membrane. *Exp Eye Res.* 1998; 66:49–67.
56. Zarbin MA. Analysis of retinal pigment epithelium integrin expression and adhesion to aged submacular human Bruch's membrane. *Trans Am Ophthalmol Soc.* 2003;101:499–520.
57. Gullapalli VK, Sugino IK, Van Patten Y, Shah S, Zarbin MA. Retinal pigment epithelium resurfacing of aged submacular human Bruch's membrane. *Trans Am Ophthalmol Soc.* 2004;102:123–137, discussion 137–128.
58. Sarks S, Cherepanoff S, Killingsworth M, Sarks J. Relationship of Basal laminar deposit and membranous debris to the clinical presentation of early age-related macular degeneration. *Invest Ophthalmol Vis Sci.* 2007;48:968–977.
59. Zheng X, Baker H, Hancock WS, Fawaz F, McCaman M, Pungor E Jr. Proteomic analysis for the assessment of different lots of fetal bovine serum as a raw material for cell culture, Part IV: application of proteomics to the manufacture of biological drugs. *Biotechnol Prog.* 2006;22:1294–1300.
60. Itaya H, Gullapalli V, Sugino IK, Tamai M, Zarbin MA. Iris pigment epithelium attachment to aged submacular human Bruch's membrane. *Invest Ophthalmol Vis Sci.* 2004;45:4520–4528.
61. Gullapalli VK, Sugino IK, Zarbin MA. Culture-induced increase in alpha integrin subunit expression in retinal pigment epithelium is important for improved resurfacing of aged human Bruch's membrane. *Exp Eye Res.* 2008;86:189–200.
62. Leonard DS, Sugino IK, Zhang XG, et al. Ultrastructural analysis of hydraulic and abrasive retinal pigment epithelial cell debridements. *Exp Eye Res.* 2003;76:473–491.
63. Underwood PA, Bennett FA. The effect of extracellular matrix molecules on the in vitro behavior of bovine endothelial cells. *Exp Cell Res.* 1993;205:311–319.
64. Gamm DM, Wang S, Lu B, et al. Protection of visual functions by human neural progenitors in a rat model of retinal disease. *PLoS ONE.* 2007;2:e338.
65. Lund RD, Wang S, Klimanskaya I, et al. Human embryonic stem cell-derived cells rescue visual function in dystrophic RCS rats. *Cloning Stem Cells.* 2006;8:189–199.
66. Lund RD, Wang S, Lu B, et al. Cells isolated from umbilical cord tissue rescue photoreceptors and visual functions in a rodent model of retinal disease. *Stem Cells.* 2007;25:602–611.
67. Lawrence JM, Keegan DJ, Muir EM, et al. Transplantation of Schwann cell line clones secreting GDNF or BDNF into the retinas of dystrophic Royal College of Surgeons Rats. *Invest Ophthalmol Vis Sci.* 2004;45:267–274.
68. Schraermeyer U, Kociok N, Heimann K. Rescue effects of IPE transplants in RCS rats: short-term results. *Invest Ophthalmol Vis Sci.* 1999;40:1545–1556.
69. Schraermeyer U, Kayatz P, Thumann G, et al. Transplantation of iris pigment epithelium into the choroid slows down the degeneration of photoreceptors in the RCS rat. *Graefes Arch Clin Exp Ophthalmol.* 2000;238:979–984.
70. Campochiaro PA, Hackett SF. Corneal endothelial cell matrix promotes expression of differentiated features of retinal pigmented epithelial cells: implication of laminin and basic fibroblast growth factor as active components. *Exp Eye Res.* 1993;57:539–547.
71. Kamei M, Kawasaki A, Tano Y. Analysis of extracellular matrix synthesis during wound healing of retinal pigment epithelial cells. *Microsc Res Tech.* 1998;42:311–316.
72. Campochiaro PA, Jerdon JA, Glaser BM. The extracellular matrix of human retinal pigment epithelial cells in vivo and its synthesis in vitro. *Invest Ophthalmol Vis Sci.* 1986;27:1615–1621.
73. Newsome DA, Pfeffer BA, Hewitt AT, Robey PG, Hassell JR. Detection of extracellular matrix molecules synthesized in vitro by monkey and human retinal pigment epithelium: influence of donor age and multiple passages. *Exp Eye Res.* 1988;46:305–321.
74. Liu X, Ye X, Yanoff M, Li W. Extracellular matrix of retinal pigment epithelium regulates choriocapillaris endothelial survival in vitro. *Exp Eye Res.* 1997;65:117–126.
75. An E, Lu X, Flippin J, et al. Secreted proteome profiling in human RPE cell cultures derived from donors with age related macular

degeneration and age matched healthy donors. *J Proteome Res.* 2006;5:2599–2610.

76. An E, Sen S, Park SK, Gordish-Dressman H, Hathout Y. Identification of novel substrates for the serine protease HTRA1 in the human RPE secretome. *Invest Ophthalmol Vis Sci.* 2010;51:3379–3386.
77. Martini B, Pandey R, Ogden TE, Ryan SJ. Cultures of human retinal pigment epithelium. Modulation of extracellular matrix. *Invest Ophthalmol Vis Sci.* 1992;33:516–521.
78. Tseng SC, Savion N, Gospodarowicz D, Stern R. Characterization of collagens synthesized by cultured bovine corneal endothelial cells. *J Biol Chem.* 1981;256:3361–3365.
79. Kay EP, Oh S. Modulation of type III collagen synthesis in bovine corneal endothelial cells. *Invest Ophthalmol Vis Sci.* 1988;29:200–207.
80. Plenz GA, Deng MC, Robenek H, Volker W. Vascular collagens: spotlight on the role of type VIII collagen in atherogenesis. *Atherosclerosis.* 2003;166:1–11.
81. Sawada H, Konomi H, Hirosawa K. Characterization of the collagen in the hexagonal lattice of Descemet's membrane: its relation to type VIII collagen. *J Cell Biol.* 1990;110:219–227.
82. Levy SG, Moss J, Sawada H, Dopping-Hepenstal PJ, McCartney AC. The composition of wide-spaced collagen in normal and diseased Descemet's membrane. *Curr Eye Res.* 1996;15:45–52.
83. Thumann G, Schraermeyer U, Bartz-Schmidt KU, Heimann K. Descemet's membrane as membranous support in RPE/IPE transplantation. *Curr Eye Res.* 1997;16:1236–1238.
84. Shaw LM, Olsen BR. FACIT collagens: diverse molecular bridges in extracellular matrices. *Trends Biochem Sci.* 1991;16:191–194.
85. Sawada H, Furthmayr H, Konomi H, Nagai Y. Immunoelectronmicroscopic localization of extracellular matrix components produced by bovine corneal endothelial cells in vitro. *Exp Cell Res.* 1987;171:94–109.
86. Klein R, Knudtson MD, Klein BE, et al. Inflammation, complement factor h, and age-related macular degeneration the multiethnic study of atherosclerosis. *Ophthalmology.* 2008;115:1742–1749.
87. Klein R. Overview of progress in the epidemiology of age-related macular degeneration. *Ophthalmic Epidemiol.* 2007;14:184–187.
88. Klein R, Klein BE, Knudtson MD, et al. Prevalence of age-related macular degeneration in 4 racial/ethnic groups in the multi-ethnic study of atherosclerosis. *Ophthalmology.* 2006;113:373–380.
89. Chang MA, Bressler SB, Munoz B, West SK. Racial differences and other risk factors for incidence and progression of age-related macular degeneration: Salisbury Eye Evaluation (SEE) Project. *Invest Ophthalmol Vis Sci.* 2008;49:2395–2402.
90. Friedman DS, Katz J, Bressler NM, Rahmani B, Tielsch JM. Racial differences in the prevalence of age-related macular degeneration: the Baltimore Eye Survey. *Ophthalmology.* 1999;106:1049–1055.
91. Bressler SB, Munoz B, Solomon SD, West SK. Racial differences in the prevalence of age-related macular degeneration: the Salisbury Eye Evaluation (SEE) Project. *Arch Ophthalmol.* 2008;126:241–245.

Supplemental Table 1. Proteins identified in BCE-ECM harvested from tissue culture dishes. Proteins are listed according to localization.

Accession Number	Protein Name	Protein MW
ECM and ECM-associated proteins		
IPI00710978	THSD4 Thrombospondin, type I, domain containing 4	19950
IPI00685669	MFAP2 Microfibrillar-associated protein 2	20695
IPI00854368	TIMP3 TIMP metallopeptidase inhibitor 3	24147
IPI00687375	TIMP3 Metalloproteinase inhibitor 3	24163
IPI00913833	LOC783816 similar to collagen triple helix repeat containing 1	25703
IPI00841285	CTHRC1 Collagen triple helix repeat containing 1	26176
IPI00807327	PSAP Pulmonary surfactant-associated protein A	26364
IPI00905635	30 kDa protein (the same as 00710978) THSD4 thrombospondin, type1, domain containing 4	29716
IPI00698668	CTGF Connective tissue growth factor	37898
IPI00706002	ANXA2 Annexin A2	38588
IPI00716158	LUM Lumican	38732
IPI00688608	DCN Decorin	39747
IPI00815631	LOC534844 similar to thrombospondin type-1 domain-containing protein 4	41545
IPI00697081	BGN Biglycan	41564
IPI00710385	ZNF280C similar to zinc finger protein 280C, partial (proline/arginine-rich end leucine-rich repeat protein)	43655
IPI00710385	PRELP Prolargin (proline/arginine-rich end leucine-rich repeat protein)	43655
IPI00701880	VWA1 von Willebrand factor A domain-containing protein 1	43711
IPI00685697	EFEMP2 EGF-containing fibulin-like extracellular matrix protein 2	49650
IPI00686824	TGFB3 TGFB3 protein (transforming growth factor, beta 3)	51287
IPI00707381	MMP11 similar to stromelysin-3	52145
IPI00712934	VTN Vitronectin	53541
IPI00907246	MMP1 54 kDa protein	53776
IPI00696930	EFEMP1 EGF-containing fibulin-like extracellular matrix protein 1	55044
IPI00906639	ECM1 60 kDa protein	60357
IPI00697984	NTN4 NTN4 protein (netrin 4)	69928
IPI00826312	NPNT similar to nephronectin precursor	71203
IPI00685504	COL8A1 Alpha 1 type VIII collagen (fragment)	73198
IPI00685447	MMP2 72 kDa type IV collagenase	73730
IPI00709922	FBLN1 FBLN1 protein (fibulin 1)	77715

Supplemental Table 1. Proteins identified in BCE-ECM harvested from tissue culture dishes. Proteins are listed according to localization.

Accession Number	Protein Name	Protein MW
IPI00690783	POSTN Periostin, osteoblast specific factor	86804
IPI00707932	COL8A2 Collagen, type VIII, alpha 2	90571
IPI00692544	EMILIN1 similar to EMILIN-1 precursor (elastin microfibril interface located protein)	106822
IPI00717179	CCDC80 CCDC80 protein (coiled-coil domain containing 80)	108157
IPI00708244	COL1A2 Collagen alpha-2(I) chain	128985
IPI00696401	Thrombospondin-1	129392
IPI00712084	THBS 1 Thrombospondin-1	129451
IPI00688802	NID1 NID1 protein (nidogen 1)	136353
IPI00731432	COL3A1 Collagen, type III, alpha 1	138354
IPI00867435	NID2 NID2 protein (nidogen 2)	142578
IPI00698002	LAMC1 similar to laminin subunit gamma-1 precursor	143111
IPI00905162	NID2 151 kDa protein	151065
IPI00729819	COL4A5 similar to alpha 5 type IV collagen isoform 2	158575
IPI00706758	COL16A1 similar to alpha 1 type XVI collagen	158944
IPI00687437	COL4A1 Collagen, type IV, alpha 1	160330
IPI00709244	COL4A3 Collagen, type IV, alpha 3	160501
IPI00912158	COL4A5 similar to alpha 5 type IV collagen isoform 1	161767
IPI00712524	COL4A2 Collagen, type IV, alpha 2, partial	164404
IPI00698418	LAMC3 similar to laminin, gamma 3	171371
IPI00824553	COL11A1 Collagen, type XI, alpha 1 isoform 4	176527
IPI00727431	TNC Tenascin C	190961
IPI00904771	LAMC1 Laminin, beta 2	196079
IPI00690076	LAMB1 Laminin B1 protein	197339
IPI00708223	AGRN similar to agrin	216327
IPI00686590	LOC100138045 similar to laminin alpha 3 subunit	229860
IPI00728194	FN1 Fibronectin 1 isoform 12	259593
IPI00714673	FN1 Embryo-specific fibronectin 1 transcript variant	262263
IPI00728875	FN1 Fibronectin	272154
IPI00711115	FBN1 Fibrillin-1	312036
IPI00714359	FBN1 313 kDa protein (fibrillin 1)	312390
IPI00709514	FBN3 similar to fibrillin 3	327863
IPI00729261	COL12A1 Collagen, type XII, alpha 1 isoform 1	351047
IPI00717460	LAMA5 similar to laminin, alpha 5	370801
IPI00713324	TNXB Tenascin-X	447103
IPI00712795	HSPG2 Heparan sulfate proteoglycan 2	467733

Supplemental Table 1. Proteins identified in BCE-ECM harvested from tissue culture dishes. Proteins are listed according to localization.

Accession Number	Protein Name	Protein MW
Secreted non-ECM Proteins		
IPI00708836	PTI Pancreatic trypsin inhibitor	10895
IPI00710453	MGP Matrix Gla protein	12217
IPI00841676	B2M similar to beta 2-microglobulin	12552
IPI00839037	PF4 13 kDa protein (platelet factor 4)	12567
IPI00867416	PF4 PF4 protein (platelet factor 4)	12601
IPI00825936	15 kDa protein	14935
IPI00685095	CST3 Cystatin-C	15799
IPI00712994	CSN2 18 kDa protein (casein beta)	18275
IPI00701640	PGLYRP1 Peptidoglycan recognition protein	21731
IPI00689257	LOC786248 similar to C4BP alpha chain (alpha spleen trypsin inhibitor, pancreatic trypsin inhibitor, complement component 4 binding protein)	22380
IPI00706094	CSN1S1 Alpha-S1-casein	24398
IPI00706501	LOX Protein-lysine 6-oxidase	24513
IPI00715174	APCS Serum amyloid P-component	25167
IPI00705441	CRP similar to C-reactive preprotein	25276
IPI00714861	C1QA Complement C1q subcomponent subunit A	25802
IPI00691707	C1QB Complement C1q subcomponent subunit B	26383
IPI00704612	RPESP RPE-spondin	29291
IPI00715548	APOA1 Apolipoprotein A-I	30258
IPI00702598	WNT5A similar to Wnt-5a isoform 1	42292
IPI00714873	PRSS23 Serine protease 23	42446
IPI00692839	SERPINE2 Serpin peptidase inhibitor, clade E (Nexin, plasminogen activator)	44002
IPI00686702	SERPINA5 Plasma serine protease inhibitor	45268
IPI00702294	SERPINE1 Plasminogen activator inhibitor 1	45342
IPI00824488	COL4A4 Collagen alpha-4(IV) chain (fragment)	46355
IPI00852486	LOX LOX protein (protein-lysine 6-oxidase precursor)	47018
IPI00707101	AHSG Alpha-2-HS-glycoprotein	47047
IPI00715866	TGFB2 Transforming growth factor beta-2	47748
IPI00706624	PCOLCE Procollagen C-endopeptidase enhancer	48080
IPI00695226	PLAU Urokinase-type plasminogen activator	48730
IPI00715339	FBLN5 Fibulin-5	50131
IPI00867362	IGHG1 protein (Ig gamma-1 chain C region)	51701
IPI00907427	SERPING1 52 kDa protein (serpin peptidase inhibitor, clade G (c1 inhibitor), member 1)	51753
IPI00690198	HPX Hemopexin	52305

Supplemental Table 1. Proteins identified in BCE-ECM harvested from tissue culture dishes. Proteins are listed according to localization.

Accession Number	Protein Name	Protein MW
IPI00688316	SERPINC1 Antithrombin-III (serpin peptidase inhibitor, clade c (antithrombin), member 1)	52314
IPI00732137	TINAGL 1 similar to tubulointerstitial nephritis antigen-like 1 isoform 2	52868
IPI00687360	SRPX2 Sushi repeat-containing protein SRPX2	53034
IPI00711678	ANGPTL2 Angiopoietin-like protein 2	56947
IPI00688367	SERPIND1 SERPIND1 protein	57071
IPI00712103	HRG Histidine-rich glycoprotein	61909
IPI00699347	HABP2 Hyaluronan-binding protein 2	62400
IPI00694104	PLAT Tissue-type plasminogen activator	63659
IPI00715828	C6H4ORF31 Chromosome 4 open reading frame 31 ortholog (fibronectin type-III domain-containing protein C4orf31 precursor)	64389
IPI00702154	LOXL1 Lysyl oxidase-like 1	64515
IPI00718725	IGHM IGHM protein (Ig mu chain C region)	65738
IPI00712538	HTRA1 HtrA serine peptidase 1	67168
IPI00700019	CFI Complement factor I	68887
IPI00708398	ALB Serum albumin	69469
IPI00710799	F2 Prothrombin (fragment)	70461
IPI00905771	QSOX1 73 kDa protein	73054
IPI00697215	F13A1 Coagulation factor XIII, A1 polypeptide	82544
IPI00700048	LOXL4 Lysyl oxidase homolog 4	83996
IPI00866946	LOXL2 LOXL2 protein (lysyl oxidase-like protein2)	86729
IPI00686012	ITIH1 Inter-alpha-trypsin inhibitor heavy chain H1	101173
IPI00717930	ITIH4 Inter-alpha-trypsin inhibitor heavy chain H4	101513
IPI00690994	ITIH5 Inter-alpha-trypsin inhibitor heavy chain H5	104292
IPI00907877	ITIH5 104 kDa protein (the same as IPI00690994)	104352
IPI00696303	LOC510360 similar to bone morphogenetic protein 1 precursor (BMP1)	105511
IPI00867404	ADAMTSL4 ADAMTSL4 protein (ADAMTS-like protein 4 precursor)	116226
IPI00730859	LTBP3 similar to latent transforming growth factor beta binding protein 3	138457
IPI00713757	CFH Complement factor H	140282
IPI00904149	A2M Alpha-2-macroglobulin	162684
IPI00713505	C3 Complement C3 (fragment)	187135
IPI00705982	LOC617696 similar to complement component 4A	192992
IPI00718698	LTBP2 Latent transforming growth factor beta binding protein 2	211448
IPI00904838	F5 222 kDa protein (coagulation factor V)	221480
Cell associated proteins (including membrane proteins)		

Supplemental Table 1. Proteins identified in BCE-ECM harvested from tissue culture dishes. Proteins are listed according to localization.

Accession Number	Protein Name	Protein MW
IPI00693947	LOC529646 similar to histone cluster 1, H2bd	13892
IPI00904598	ITGA3 Putative uncharacterized protein (fragment)	14611
IPI00698263	LOC524269 similar to ribosomal protein S15a	14840
IPI00710783	HBA1; HBA2 Hemoglobin subunit alpha	15175
IPI00827107	LOC781088; LOC781674; LOC783672 similar to gamma globin	15806
IPI00715405	HBG; LOC788610 Hemoglobin fetal subunit beta	15849
IPI00904417	LOC789582 similar to endoplasmic reticulum-golgi intermediate compartment 3	16648
IPI00718271	MYL6 Isoform non-muscle of myosin light polypeptide 6	16919
IPI00703665	RAP1A Ras-related protein Rap-1A	20856
IPI00838711	CAV1 Caveolin (fragment)	21484
IPI00717110	PGRMC1 Membrane-associated progesterone receptor component 1	21609
IPI00708597	ARL6IP5 PRA1 family protein 3	21651
IPI00694243	RPS7 40S ribosomal protein S7	22127
IPI00700655	MGC137211 Putative uncharacterized protein MGC137211	22780
IPI00687416	RRAS2 RRAS2 protein (Ras-related protein R-Ras2 precursor)	23385
IPI00686645	CD9 CD9 antigen	25127
IPI00718388	AQP1 Aquaporin-1	28782
IPI00714181	RPL7 60S ribosomal protein L7	29169
IPI00868611	ARVCF ARVCF protein	31579
IPI00724774	LOC781724 similar to ribosomal protein L6-like	32638
IPI00689722	CD80 anitgen (fragment)	33048
IPI00807279	CD47 CD47 molecule	33289
IPI00713885	AHSA1 AHA1, activator of heat shock 90kDa protein ATPase homolog 1	38241
IPI00847093	RCN1 RCN1 protein	38728
IPI00838220	CD55 DAF-2 (complement decay-accelerating factor precursor)	40972
IPI00701659	BOLA Class I histocompatibility antigen, alpha chain BL3-7	41487
IPI00698900	ACTB Actin, cytoplasmic 1	41737
IPI00712838	ACTG1 Actin, cytoplasmic 2	41766
IPI00906529	ACTC1 42 kDa protein	42000
IPI00688489	ACTC1 Actin, alpha cardiac muscle 1	42019
IPI00825112	GNAQ Guanine nucleotide binding protein (G protein), q polypeptide	42142
IPI00710378	KRT7 45 kDa protein	44953

Supplemental Table 1. Proteins identified in BCE-ECM harvested from tissue culture dishes. Proteins are listed according to localization.

Accession Number	Protein Name	Protein MW
IPI00710821	LOC521214 similar to MGC152498 protein	46247
IPI00694938	SERPINH1 Serpin H1	46477
IPI00685656	KRT31 Keratin 31	47043
IPI00714052	ACTR3 Actin-related protein 3	47371
IPI00709301	LOC507271 similar to ribosomal protein L4 isoform 2	47396
IPI00689638	MFGE8 MFGE8 protein (milk fat globule-EGF factor 8 protein)	47831
IPI00706594	TUBB2C Tubulin beta-2C chain	49700
IPI00704353	TUBA4A Tubulin alpha-4A chain	49793
IPI00712127	TUBB6 Tubulin beta-6 chain	49868
IPI00691086	SLC29A1 Solute carrier family 29 (nucleoside transporters), member 1	50219
IPI00701878	SRPX Sushi-repeat-containing protein, X-linked	50830
IPI00694214	KRT7 Keratin, type II cytoskeletal 7	51578
IPI00721270	KRT19 Keratin 19 isoform 8	51849
IPI00698174	BECN1 Beclin-1	51896
IPI00689228	VIM Vimentin	53695
IPI00845209	KRT83 Keratin, type II cuticular Hb3	53955
IPI00693601	SLC2A3 Solute carrier family 2 (facilitated glucose transporter), member 3	54083
IPI00907118	SLC2A1 54 kDa protein (solute carrier family 2, facilitated glucose transporter member 1)	54099
IPI00714656	SLC2A1 Solute carrier family 2, facilitated glucose transporter member 1	54132
IPI00911907	LOC100138974 Keratin 10 (Epidermolytic hyperkeratosis)	54816
IPI00714315	KRT10 Keratin, type I cytoskeletal 10	54849
IPI00698285	KRT24 similar to keratin, type I cytoskeletal 24	55095
IPI00707203	SLC16A9 similar to solute carrier family 16 (monocarboxylic acid transporters), member 9	55794
IPI00715687	KRT85 Keratin 85	55860
IPI00709465	P4HB Protein disulfide-isomerase	57230
IPI00716415	C keratin 6C isoform 2	58860
IPI00690217	GPC4 similar to glypican 4	62376
IPI00726805	SLC22A5 Solute carrier family 22 (organic cation/carnitine transporter), member 5	62785
IPI00867237	QSOX1 QSOX1 protein (sulfhydryl oxidase 1 precursor)	62935
IPI00824847	KRT2 similar to keratin 2	63866
IPI00716748	BCAM Lutheran glycoprotein	68003

Supplemental Table 1. Proteins identified in BCE-ECM harvested from tissue culture dishes. Proteins are listed according to localization.

Accession Number	Protein Name	Protein MW
IPI00694641	EZR Ezrin	69413
IPI00716785	CPT2 Carnitine O-palmitoyltransferase 2, mitochondrial	74483
IPI00699890	CD276 CD276 molecule	77060
IPI00708219	CAPN1 Calpain-1 catalytic subunit	82207
IPI00700542	AEBP1 Transcription factor AEBP1	82314
IPI00703837	RPS6KA2 similar to ribosomal protein S6 kinase, 90kDa, polypeptide 2	82975
IPI00688236	CTNNB1 Catenin beta-1	85497
IPI00840544	JUP 86 kDa protein	85616
IPI00760525	ITGB1 Isoform 2 of integrin beta-1	88433
IPI00698144	SULF2 similar to sulfatase 2 isoform 2	99754
IPI00904503	CLTC Protein	103668
IPI00713468	ACTN4 Alpha-actinin-4	104928
IPI00703243	GANAB Glucosidase, alpha; neutral AB	109341
IPI00703753	ENPP1 similar to ecto-nucleotide pyrophosphatase/phosphodiesterase 1	112344
IPI00705159	ATP1A1 Sodium/potassium-transporting ATPase subunit alpha-1	112568
IPI00709893	ATP1A1 Sodium/potassium-transporting ATPase alpha-1 chain	112725
IPI00692144	NNT NAD(P) transhydrogenase, mitochondrial	113896
IPI00905418	ITGA3 116 kDa protein (integrin alpha-3 precursor)	116333
IPI00712829	DCLRE1A similar to DNA cross-link repair 1A	118314
IPI00691262	FARP1 similar to FERM, RhoGEF, and pleckstrin domain protein 1	118633
IPI00698007	SLC4A4 Electrogenic sodium bicarbonate cotransporter 1	121461
IPI00717432	PLCL2 similar to inactive phospholipase C-like protein 2	124673
IPI00907270	TBCD TBCD protein	129966
IPI00697727	KERIV Cytokeratin type II, component IV isoform 3	132763
IPI00704893	GAPVD1 GTPase-activating protein and VPS9 domain-containing protein 1	157277
IPI00696012	MYH9 Non-muscle myosin heavy chain	227461
IPI00703832	MYOF similar to myoferlin isoform 12	234511
IPI00694504	TNC 244 kDa protein (tenascin precursor)	244333
IPI00694670	CELSR1 similar to cadherin EGF LAG seven-pass G-type receptor 1	333741
IPI00692492	ATM similar to ataxia telangiectasia mutated protein	350306
IPI00700318	LOC534358 similar to putative utrophin	403273

Supplemental Table 1. Proteins identified in BCE-ECM harvested from tissue culture dishes. Proteins are listed according to localization.

Accession Number	Protein Name	Protein MW
IPI00687372	ALCAM CD166 antigen	504803
Unknown		
IPI00905271	8 kDa protein	7972
IPI00709002	29 kDa protein	29331
IPI00688092	MGC151567 Putative uncharacterized protein MGC151567	34435
IPI00907510	36 kDa protein	36304
IPI00824136	LOC784007 similar to LOC496253 protein	41900
IPI00714264	IGHM 53 kDa protein	52890
IPI00688825	LOC100125300 Coiled-coil domain-containing protein KIAA1656 homolog	70529
IPI00693021	CCDC40 similar to coiled-coil domain containing 40	146645
IPI00686565	192 kDa protein	192338
IPI00687057	LOC528008 hypothetical protein	262647
IPI00686143	383 kDa protein	382876
IPI00704118	505 kDa protein	504472